

Non-Markovian Dynamics of the Spin-Boson Model

Pro gradu -tutkielma
Turun yliopisto
Teoreettinen fysiikka
2009
LuK Elsi Laine
Tarkastajat:
Dos. Jyrki Piilo
Prof. Kalle-Antti Suominen

Contents

Introduction	1
1 Markovian and Non-Markovian Dynamics of Open Quantum Systems	3
1.1 Reduced Dynamics	3
1.2 Markovian Master Equation	5
1.2.1 Perturbative Calculation of the Master Equation	6
1.2.2 Assumptions of the Reservoir	7
1.3 Non-Markovian Master Equation and Projection Operator Techniques	11
1.3.1 Nakajima-Zwanzig Equation	13
1.3.2 Time-Convolutionless Projecton Operator Method	16
1.3.3 Perturbative Treatment of the Equations	18
2 The Spin-Boson Model	20
2.1 Derivation of the Master Equation	21
2.1.1 Calculation of the Eigenoperators	22
2.1.2 Determining the Decay Rates	23
2.2 Numerical Solution to the Master Equation	28
2.3 Special Cases	30
2.3.1 Limit of Pure Dephasing, No Tunneling	31
2.3.2 Tunneling Dynamics, Zero Energy Bias	34
2.3.3 Markovian Case	37
2.4 Validity of the Secular Approximation	38
3 Quantum-Jump Approach to Open System Dynamics	41
3.1 Monte Carlo Wave-Function Method and Markovian Quantum Jumps	42
3.2 Non-Markovian Quantum Jumps	46
3.3 Non-Markovian Quantum Jumps and the Spin-Boson Model	49
4 Applications for the spin-boson model	58
4.1 Double-well system	58
4.2 Double quantum dot charge qubit	60

4.2.1	Double Dot Model	61
4.2.2	Boson Spectral Density	62
4.3	Biomolecular systems and the Spin-Boson Model	64
4.3.1	Model for Individual Chromophores with the Solvent	64
4.3.2	Model for Two Biomolecules	65
5	Conclusions	68

Introduction

The spin-boson model describes a two-level system interacting with a reservoir described by a bath of harmonic oscillators. Many physical systems can be approximated by a two-level system in the low-temperature limit, where higher excitations are neglected [1]. Thus, the spin-boson model has played a major role in understanding the dissipative dynamics in quantum systems [2].

The spin-boson model is widely studied, mostly because of its many applications in the field of quantum information theory and chemistry. The model can describe for example a simple two-well potential [3], double quantum dots [4] and different biomolecular systems [5, 6]. Because the spin-boson model is not exactly solvable many approximative approaches have been used in order to unravel the dynamics of the spin-boson system. The model has been studied using perturbation theory in the system-environment coupling with the Markov approximation [7, 8] and projection operator methods [9]. In reference [3] an approximative scheme called the interacting blip approximation (NIBA) has been introduced. It is a perturbative approach in the tunneling matrix element based on path integral methods. In reference [10] it is shown that the NIBA approach is equivalent with a projection operator method in the weak tunneling approximation. There also exists an exact approach to the problem using Feynman-Vernon path integral method [11, 12]. However, this presents only a formal solution.

Understanding the short-time dynamics of the spin-boson model is crucial in understanding quantum computing systems [13, 14]. The Markovian approximation is valid only for long times and thus the non-Markovian description of the dynamics is needed. NIBA fails for large tunneling matrix element and cannot therefore be applied to biomolecular systems [5, 6]. Many projection operator methods and path integral methods are difficult to treat and do not necessarily give much physical insight to the problem.

First part of the thesis is focused on general description of open quantum systems and the concepts of reduced system dynamics and master equation. A common feature for non-Markovian open systems is the memory preserved in the environment. To describe the memory effects the master equation needs to be derived in the absence of Markovian approximation. A projection operator technique is presented in order to derive a time-convolutionless non-Markovian master equation [1]. The goal of this thesis is to write a time-convolutionless non-Markovian master equation describing the reduced system dynamics of the spin-boson model. The master equation is derived in second order and the secular approximation is performed. The derived master equation can then be unraveled via the theory of non-Markovian quantum jumps [15].

In the last chapter physical applications for the spin-boson model are studied. The truncation procedure reducing a double-well system into a two-state system and two types of physical realizations of qubits are introduced. The other qubit realization uses mesoscopic semiconductor structures and the other optically active biomolecules. It is shown that the spin-boson model describes the essential dynamics of these systems.

Chapter 1

Markovian and Non-Markovian Dynamics of Open Quantum Systems

A quantum system is never entirely isolated from its surroundings. As in classical physics, any realistic system is coupled to an environment which influences the dynamics of the system. Also, any empirical test of a quantum system requires one to couple it to a measuring apparatus which influences the object being measured. Thus, it is essential to study quantum systems interacting with an environment. Such a system without ignorable coupling to the environment is called open quantum system. Throughout this thesis we put $\hbar = 1$.

1.1 Reduced Dynamics

Assume an open quantum system (\mathcal{S}) interacting with a large environment (\mathcal{E}) such that the composite system ($\mathcal{S} + \mathcal{E}$) is closed. The possibility of identification of such an environment is an essential presupposition in the methodology of physics [16]. Now that the composite system is closed the dynamics is deterministic. The family of maps $\{V(t)|t \geq 0\}$ describing the evolution of the composite system ($|\psi(t)\rangle =$

$V_t |\psi(0)\rangle\rangle$ is a dynamical group. The theorems of Wigner and Stone [17, 18] ensure that one can write the Schrödinger equation describing the evolution of a state vector of the total system

$$i \frac{d}{dt} |\psi(t)\rangle = H(t) |\psi(t)\rangle, \quad (1.1)$$

where $H(t)$ is the Hamiltonian of the composite system. The solution of the Schrödinger equation (1.1) can be represented in terms of a unitary operator [19]

$$U(t, t_0) = I + \sum_{n=1}^{\infty} (-i)^n \int \int \cdots \int H(t_1) \cdots H(t_n) dt_n \cdots dt_1. \quad (1.2)$$

If the system is in a mixed state the corresponding quantum statistical ensemble may be characterized with the help of a statistical operator or a density matrix ρ [1]. The equation of motion for the density matrix of the total system is

$$\frac{d}{dt} \rho(t) = -i[H(t), \rho(t)], \quad (1.3)$$

which is called the Liouville-von Neumann equation.

Denoting the Hilbert space of the system \mathcal{H}_S and of the environment \mathcal{H}_E the Hilbert space of the total system is the tensor product space $\mathcal{H}_S \otimes \mathcal{H}_E$. If the free evolution Hamiltonian ($H_S \otimes I_E + I_S \otimes H_E$) is assumed to be time-independent, the Hamiltonian of the composite system ($\mathcal{S} + \mathcal{E}$) can be written as

$$H(t) = H_S \otimes I_E + I_S \otimes H_E + H_I(t). \quad (1.4)$$

Here, H_S is the system free Hamiltonian, H_E is the environment free Hamiltonian and H_I is the Hamiltonian describing the interaction between the system and the environment. The equation of motion for the reduced density operator describing the evolution of the system (\mathcal{S}) is obtained by taking a partial trace over the environment on both sides in equation (1.3):

$$\frac{d}{dt} \rho_S(t) = -i \text{tr}_E [H(t), \rho(t)]. \quad (1.5)$$

1.2 Markovian Master Equation

In general, it is impossible to calculate the reduced density operator from (1.5) exactly. A common approximation performed in order to solve the reduced density operator is the Markov approximation, in which the memory effects of the environment are neglected. This can be formulated in terms of a semigroup property [20].

Assuming that the initial state of the total system is of the form $\rho(0) = \rho_S(0) \otimes \rho_E(0)$ ¹, the dynamics of the open system is presented by a map in the state space of the system:

$$\rho_S(0) \mapsto \rho_S(t) = V(t)\rho_S(0). \quad (1.6)$$

For a fixed time t this map is referred to as a dynamical map. These maps provide a one parameter family $\{V(t)|t \geq 0\}$. If the memory effects of the reduced system dynamics are neglected, the dynamics is Markovian [21] and the dynamical map has the semigroup property

$$V(t_1 + t_2) = V(t_1)V(t_2), \quad t_1, t_2 \geq 0. \quad (1.7)$$

This property makes the one parameter family of dynamical maps a quantum dynamical semigroup. There exists a generator \mathcal{L} defined as $V(t) = e^{\mathcal{L}t}$ [20] which determines the equation of motion for the reduced density operator:

$$\frac{d}{dt}\rho_S(t) = \mathcal{L}\rho_S(t). \quad (1.8)$$

This is called the Markovian master equation. The most general form of the generator \mathcal{L} is provided by a theorem of Gorini, Kossakowski and Sudarshan [22] and a theorem of Lindblad [23]. It is written as

$$\mathcal{L}\rho_S = -i[H_C, \rho_S] + \sum_i \gamma_i (A_i \rho_S A_i^\dagger - \frac{1}{2} \{A_i^\dagger A_i, \rho_S\}), \quad (1.9)$$

¹This is a reasonable assumption when the coupling between the system and the environment is weak.

where H_C is the Hamiltonian of the coherent part of the evolution and A_i s are system operators with corresponding relaxation rates γ_i . In the next chapter this form of a master equation is derived from the microscopic theory under certain assumptions. The microscopic derivation of the Markovian master equation presented in the next two sections is mostly based on references [1, 24].

1.2.1 Perturbative Calculation of the Master Equation

Let the total Hamiltonian be as in (1.4) and $H_0 = H_S + H_E$. The density operator of the total system is described by the Liouville-von Neumann equation (1.3). Written in the interaction picture the equation is

$$\frac{d}{dt}\tilde{\rho}(t) = -i[\tilde{H}_I(t), \tilde{\rho}(t)] \quad (1.10)$$

with

$$\begin{aligned} \tilde{\rho}(t) &= e^{iH_0t}\rho(t)e^{-iH_0t}, \\ \tilde{H}_I(t) &= e^{iH_0t}H_Ie^{-iH_0t}. \end{aligned} \quad (1.11)$$

One can perform a formal integration of equation (1.10). This yields

$$\tilde{\rho}(t) - \tilde{\rho}(t_0) = -i \int_{t_0}^t [\tilde{H}_I(t'), \tilde{\rho}(t')] dt'. \quad (1.12)$$

Inserting this back to (1.10) one can write the differential equation in the form

$$\frac{d}{dt}\tilde{\rho}(t) = -i[\tilde{H}_I(t), \tilde{\rho}(t_0)] + (-i)^2 \int_{t_0}^t [\tilde{H}_I(t), [\tilde{H}_I(t'), \tilde{\rho}(t')]] dt'. \quad (1.13)$$

Continuing iteratively the equation can be written as

$$\begin{aligned} \frac{d}{dt}\tilde{\rho}(t) &= -i[\tilde{H}_I(t), \tilde{\rho}(t_0)] + (-i)^2 \int_{t_0}^t [\tilde{H}_I(t), [\tilde{H}_I(t'), \tilde{\rho}(t_0)]] dt' \\ &\quad + (-i)^3 \int_{t_0}^t \int_{t_0}^{t'} [\tilde{H}_I(t), [\tilde{H}_I(t'), [\tilde{H}_I(t''), \tilde{\rho}(0)]]] dt'' dt' + \dots \end{aligned} \quad (1.14)$$

Assuming that the interaction is sufficiently small one can neglect higher than second order terms in the expansion. Now

$$\frac{d}{dt}\tilde{\rho}(t) = -i[\tilde{H}_I(t), \tilde{\rho}(t_0)] + (-i)^2 \int_{t_0}^t [\tilde{H}_I(t), [\tilde{H}_I(t'), \tilde{\rho}(t_0)]] dt'. \quad (1.15)$$

One can assume factorized initial conditions $\tilde{\rho}(t_0) = \tilde{\rho}_S(t_0) \otimes \tilde{\rho}_E(t_0)$ due to the weak-coupling approximation performed earlier [31]. By taking the partial trace over the degrees of freedom of the reservoir one obtains a differential equation for the reduced density operator

$$\begin{aligned} \frac{d}{dt}\tilde{\rho}_S(t) &= -i\text{tr}_E[\tilde{H}_I(t), \tilde{\rho}_S(t_0) \otimes \tilde{\rho}_E(t_0)] \\ &+ (-i)^2 \int_{t_0}^t \text{tr}_E[\tilde{H}_I(t), [\tilde{H}_I(t'), \tilde{\rho}_S(t_0) \otimes \tilde{\rho}_E(t_0)]] dt'. \end{aligned} \quad (1.16)$$

One can write the integral form of equation (1.16) and solve $\tilde{\rho}_S(0)$. Now, by substituting this back into equation (1.16) and by neglecting higher than second order terms one can write the master equation in the following form:

$$\begin{aligned} \frac{d}{dt}\tilde{\rho}_S(t) &= -i\text{tr}_E[\tilde{H}_I(t), \tilde{\rho}_S(t) \otimes \tilde{\rho}_E(t_0)] \\ &- (-i)^2 \int_{t_0}^t \text{tr}_E[\tilde{H}_I(t), \text{tr}_E[\tilde{H}_I(t'), \tilde{\rho}_S(t_0) \otimes \tilde{\rho}_E(t_0)]] \otimes \tilde{\rho}_E(t_0) dt' \\ &+ (-i)^2 \int_{t_0}^t \text{tr}_E[\tilde{H}_I(t), [\tilde{H}_I(t'), \tilde{\rho}_S(t) \otimes \tilde{\rho}_E(t)]] dt'. \end{aligned} \quad (1.17)$$

1.2.2 Assumptions of the Reservoir

Since the reservoir is assumed to be much larger than the system the variation of $\tilde{\rho}_E(t)$ due to the coupling with the system is weak. Thus, it is justified to assume that

$$\tilde{\rho}_E(t) \simeq \tilde{\rho}_E(t_0) = \rho_E. \quad (1.18)$$

Thus the equation (1.17) may be written as

$$\begin{aligned} \frac{d}{dt}\tilde{\rho}_S(t) &= -i\text{tr}_\mathcal{E}[\tilde{H}_I(t), \tilde{\rho}_S(t) \otimes \rho_\mathcal{E}] \\ &\quad -(-i)^2 \int_{t_0}^t \text{tr}_\mathcal{E}[\tilde{H}_I(t), \text{tr}_\mathcal{E}[\tilde{H}_I(t'), \tilde{\rho}_S(t_0) \otimes \tilde{\rho}_\mathcal{E}] \otimes \tilde{\rho}_\mathcal{E}] dt' \\ &\quad +(-i)^2 \int_{t_0}^t \text{tr}_\mathcal{E}[\tilde{H}_I(t), [\tilde{H}_I(t'), \tilde{\rho}_S(t) \otimes \rho_\mathcal{E}]] dt'. \end{aligned} \quad (1.19)$$

The interaction Hamiltonian H_I is taken to be a tensor product of observable S of the system \mathcal{S} and an observable E of the environment \mathcal{E} .

$$H_I = S \otimes E, \quad (1.20)$$

which in the interaction picture gives

$$\tilde{H}_I(t) = \tilde{S}(t) \otimes \tilde{E}(t), \quad (1.21)$$

where

$$\begin{aligned} \tilde{S}(t) &= e^{iH_S t} S e^{-iH_S t}, \\ \tilde{E}(t) &= e^{iH_E t} E e^{-iH_E t}. \end{aligned} \quad (1.22)$$

Assuming that the average value of the observable E in state $\rho_\mathcal{E}$ is zero it follows that

$$\text{tr}_\mathcal{E}[\rho_\mathcal{E} \tilde{H}_I(t)] = 0 \quad (1.23)$$

and therefore the two first terms in equation (1.19) disappear. Now the dynamics of the reduced density matrix can be written in the form

$$\frac{d}{dt}\tilde{\rho}_S(t) = - \int_{t_0}^t dt' \text{tr}_\mathcal{E}[\tilde{H}_I(t), [\tilde{H}_I(t'), \tilde{\rho}_S(t) \otimes \rho_\mathcal{E}]]. \quad (1.24)$$

Inserting the factorized \tilde{H}_I (1.21) into equation (1.24) yields

$$\begin{aligned} \frac{d}{dt}\tilde{\rho}_S(t) &= - \int_{t_0}^t dt' \left[\text{tr}_\mathcal{E} \left\{ \tilde{E}(t) \tilde{E}(t') \rho_\mathcal{E} \right\} \left[\tilde{S}(t) \tilde{S}(t') \rho_S(t) - \tilde{S}(t') \rho_S(t) \tilde{S}(t) \right] \right. \\ &\quad \left. + \text{tr}_\mathcal{E} \left\{ \tilde{E}(t) \tilde{E}(t') \rho_\mathcal{E} \right\} \left[\rho_S(t) \tilde{S}(t') \tilde{S}(t) - \tilde{S}(t) \rho_S(t) \tilde{S}(t') \right] \right]. \end{aligned} \quad (1.25)$$

Substituting the integration variable t' by $t - t'$ yields

$$\begin{aligned} \frac{d}{dt}\tilde{\rho}_S(t) = & - \int_0^{t-t_0} dt' \left[\text{tr}_\mathcal{E} \left\{ \tilde{E}(t)\tilde{E}(t-t')\rho_\mathcal{E} \right\} \times \right. \\ & \left[\tilde{S}(t)\tilde{S}(t-t')\rho_S(t) - \tilde{S}(t-t')\rho_S(t)\tilde{S}(t) \right] \\ & \left. + \text{tr}_\mathcal{E} \left\{ \tilde{E}(t)\tilde{E}(t-t')\rho_\mathcal{E} \right\} \left[\rho_S(t)\tilde{S}(t-t')\tilde{S}(t) - \tilde{S}(t)\rho_S(t)\tilde{S}(t-t') \right] \right]. \end{aligned} \quad (1.26)$$

The terms

$$\left\langle \tilde{E}(t)\tilde{E}(t-t') \right\rangle = \text{tr}_\mathcal{E} \left\{ \tilde{E}(t)\tilde{E}(t-t')\rho_\mathcal{E} \right\} \quad (1.27)$$

describe the correlations of the reservoir. These reservoir correlation functions are homogeneous in time i.e.

$$\left\langle \tilde{E}(t)\tilde{E}(t-t') \right\rangle = \left\langle \tilde{E}(t')\tilde{E}(0) \right\rangle. \quad (1.28)$$

Thus, the master equation is

$$\begin{aligned} \frac{d}{dt}\tilde{\rho}_S(t) = & - \int_0^{t-t_0} dt' \left[\text{tr}_\mathcal{E} \left\{ \tilde{E}(t')\tilde{E}(0)\rho_\mathcal{E} \right\} \times \right. \\ & \left[\tilde{S}(t)\tilde{S}(t-t')\rho_S(t) - \tilde{S}(t-t')\rho_S(t)\tilde{S}(t) \right] \\ & \left. + \text{tr}_\mathcal{E} \left\{ \tilde{E}(t')\tilde{E}(0)\rho_\mathcal{E} \right\} \left[\rho_S(t)\tilde{S}(t-t')\tilde{S}(t) - \tilde{S}(t)\rho_S(t)\tilde{S}(t-t') \right] \right]. \end{aligned} \quad (1.29)$$

If the time $t - t_0$ is much larger than the reservoir correlation time τ_B one can put the upper limit of the integral to infinity because the correlation functions $\text{tr}_\mathcal{E} \left\{ \tilde{E}(t')\tilde{E}(0)\rho_\mathcal{E} \right\}$ are negligible after time τ_B and thus no remarkable error is made if the domain of integration is changed. This approximation is referred to as the Markovian approximation. Now for $t \gg \tau_B$

$$\begin{aligned} \frac{d}{dt}\tilde{\rho}_S(t) = & - \int_0^\infty dt' \left[\text{tr}_\mathcal{E} \left\{ \tilde{E}(t')\tilde{E}(0)\rho_\mathcal{E} \right\} \left[\tilde{S}(t)\tilde{S}(t-t')\rho_S(t) - \tilde{S}(t-t')\rho_S(t)\tilde{S}(t) \right] \right. \\ & \left. + \text{tr}_\mathcal{E} \left\{ \tilde{E}(t')\tilde{E}(0)\rho_\mathcal{E} \right\} \left[\rho_S(t)\tilde{S}(t-t')\tilde{S}(t) - \tilde{S}(t)\rho_S(t)\tilde{S}(t-t') \right] \right]. \end{aligned} \quad (1.30)$$

To make it easier to carry out the secular approximation one can decompose the the system operator S in the interaction Hamiltonian H_I into eigenoperators of the

system Hamiltonian H_S . The system operator S can be written as

$$S = \sum_{\omega} S(\omega), \quad (1.31)$$

where $\omega = \epsilon' - \epsilon$ with ϵ' and ϵ being the eigenvalues of the system Hamiltonian H_S . The system eigenoperators are defined as

$$S(\omega) \equiv \sum_{\epsilon' - \epsilon = \omega} \Pi(\epsilon) S \Pi(\epsilon'), \quad (1.32)$$

where $\Pi(\epsilon)$ denotes the projection onto the eigenspace belonging to the eigenvalue ϵ . By inserting the decomposition (1.31) into equation (1.30) one obtains

$$\frac{d}{dt} \tilde{\rho}_S(t) = \sum_{\omega, \omega'} e^{i(\omega' - \omega)t} \Gamma(\omega) [S(\omega) \rho_S S^\dagger(\omega') - S^\dagger(\omega') S(\omega) \rho_S(t)] + h.c. \quad (1.33)$$

Here, $h.c$ means the Hermitean conjugated expression and

$$\Gamma(\omega) \equiv \int_0^\infty dt' e^{i\omega t'} \text{tr}_{\mathcal{E}} \left\{ \tilde{E}^\dagger(t) \tilde{E}(t - t') \rho_{\mathcal{E}} \right\} = \int_0^\infty dt' e^{i\omega t'} \text{tr}_{\mathcal{E}} \left\{ \tilde{E}^\dagger(t') \tilde{E}(0) \rho_{\mathcal{E}} \right\}. \quad (1.34)$$

To attain a master equation in Lindblad form (1.9) the secular approximation [1] can be performed in the master equation (1.33). Essentially, the secular approximation consists of replacing the generator of the interaction picture master equation by its time average. The typical time scale of the system is defined as a typical value of $|\omega' - \omega|^{-1}$ when $\omega \neq \omega'$. If the typical time scale of the system τ_S is much smaller than the relaxation time of the system τ_R the terms in (1.33) in which $\omega' \neq \omega$ can be neglected since they oscillate very rapidly during the time τ_R . Assuming the preceding type of time scales for the system and defining $\Gamma(\omega) \equiv \frac{1}{2}\gamma(\omega) + i\lambda(\omega)$ the equation (1.33) can be written in the form

$$\dot{\rho}_S(t) = -i[H_{LS}, \tilde{\rho}_S(t)] + \mathcal{D}(\tilde{\rho}_S(t)), \quad (1.35)$$

where

$$H_{LS} = \sum_{\omega} \lambda(\omega) S^\dagger(\omega) S(\omega) \quad (1.36)$$

and

$$\mathcal{D}(\tilde{\rho}_S(t)) = \sum_{\omega} \gamma(\omega) \left[S(\omega) \tilde{\rho}_S S^\dagger(\omega) - \frac{1}{2} \{ S^\dagger(\omega) S(\omega), \tilde{\rho}_S \} \right]. \quad (1.37)$$

The generator of this master equation is in the Lindblad form (1.9). It thus provides a quantum dynamical semigroup.

1.3 Non-Markovian Master Equation and Projection Operator Techniques

In the previous chapter a master equation was derived in the case of a Markovian system which does not have memory in the meaning that the information the system loses to its environment does not affect the future system dynamics. In the case of environment with non-trivial structure, the information lost earlier to the reservoir is fed back to the system. This information return causes non-Markovian dynamics with memory. Then the dynamics is not mathematically described by a dynamical semigroup and the generator \mathcal{L} is not in general in the Lindblad form (1.9).

Projection operator methods provide a powerful tool in deriving equations describing the reduced dynamics. The projection operator method described in section 1.3.1 yields an exact integro-differential equation, called the Nakajima-Zwanzig equation [25, 26], describing the non-Markovian dynamics of an open system. An integro-differential equation is rather difficult to treat so it would be more convenient to have a time-convolutionless form of the master equation. A time-convolutionless master equation is local-in-time and thus easier to treat than equations with a memory kernel.

In section 1.3.2 a time-convolutionless master equation is derived by using the time-convolutionless operator method (TCL). When the equation is approximated in second order one can perform the secular approximation which leads to a master

equation of the form which is very similar to the Lindblad form (1.9), but with time-dependent and possibly temporarily negative decay rates. What has been often misunderstood (c.f. [27]) is that although being local in time, the master equation derived using the time convolutionless projection operator method does possess the memory effects present in the memory kernel of the Nakajima-Zwanzig equation. The memory effects can be demonstrated by unraveling the master equation with the non-Markovian quantum jump method presented in section 3 [28] or by studying a non-Markovian stochastic Schrödinger equation in which the memory effects are present in statistical correlations between different realizations of the process [29].

In the case of a Markovian master equation the Lindblad form guarantees that the system density matrix is physical: it is of trace one, Hermitian and positive. This result can also be generalized into a case of time-dependent Markovian case, i.e. to the case with time-dependent positive decay rates [30]. In the case of non-Markovian dynamics there does not exist a general form of the master equation guaranteeing the physicality of the density matrix. When the positivity of the density matrix is broken, the master equation fails to describe the system dynamics.

The idea of projection operator techniques is to identify the operation of tracing over the environment as a projection $\rho \mapsto \mathcal{P}\rho$ in the state space of the total system. The state space operator \mathcal{P} is a projection operator, i.e. $\mathcal{P}^2 = \mathcal{P} = \mathcal{P}^\dagger$. The density matrix $\mathcal{P}\rho$ is called the relevant part of the total system density operator ρ . The orthogonal projection of \mathcal{P} is defined as $\mathcal{Q} = I - \mathcal{P}$. The density matrix $\mathcal{Q}\rho$ is called the irrelevant part of the density operator ρ . The aim is to derive an equation of motion for the relevant part $\mathcal{P}\rho$. The next two sections are based on the approaches in [1] and [31].

1.3.1 Nakajima-Zwanzig Equation

An open system \mathcal{S} coupled to an environment \mathcal{E} is described by a Hamiltonian of the form

$$H = H_0 + \alpha H_I, \quad (1.38)$$

where H_0 is the free Hamiltonian of the system and environment, H_I describes the interaction between the system and the environment and α is a dimensionless expansion parameter. The expansion parameter α determines the strength of the interaction H_I with respect to the free dynamics H_0 . In the interaction picture, the equation of motion for the density matrix of the composite system reads

$$\frac{d}{dt}\rho(t) = -i\alpha \left[\tilde{H}_I(t), \tilde{\rho}(t) \right] \equiv \alpha \mathcal{L}(t)\tilde{\rho}(t), \quad (1.39)$$

where the density matrix and the interaction Hamiltonian in the interaction picture are

$$\begin{aligned} \tilde{\rho}(t) &= e^{iH_0 t} \rho(t) e^{-iH_0 t}, \\ \tilde{H}_I(t) &= e^{iH_0 t} H_I e^{-iH_0 t}. \end{aligned} \quad (1.40)$$

In order to derive an equation of motion for the reduced density matrix the projection operator acting in the state space is defined as

$$\tilde{\rho} \mapsto \mathcal{P}\tilde{\rho} = \text{tr}_{\mathcal{E}} \{ \tilde{\rho} \} \otimes \tilde{\rho}_{\mathcal{E}} = \tilde{\rho}_{\mathcal{S}}(t) \otimes \tilde{\rho}_{\mathcal{E}}, \quad (1.41)$$

where $\tilde{\rho}_{\mathcal{E}}$ is a given reference state of the environment. The orthogonal projection of \mathcal{P} is

$$\mathcal{Q}\tilde{\rho} = \tilde{\rho} - \mathcal{P}\tilde{\rho}, \quad (1.42)$$

where \mathcal{P} and \mathcal{Q} are called the relevant and irrelevant part of the density operator respectively. It is assumed that $\tilde{\rho}_{\mathcal{E}}$ is normalized. It is easy to check that \mathcal{P} and \mathcal{Q}

are indeed projection operators and thus have the properties

$$\mathcal{P} + \mathcal{Q} = I, \quad (1.43)$$

$$\mathcal{P}^2 = \mathcal{P}, \quad (1.44)$$

$$\mathcal{Q}^2 = \mathcal{Q}, \quad (1.45)$$

$$\mathcal{P}\mathcal{Q} = \mathcal{Q}\mathcal{P} = 0. \quad (1.46)$$

The choice of the reference state depends on the application under consideration. It is usually chosen as a thermal state of the environment but in general the specification of the reference state is quite subtle [31]. In the following it is assumed that $\tilde{\rho}_{\mathcal{E}}$ is time independent. We also make a technical assumption that the odd moments of the interaction Hamiltonian with respect to the reference state vanish, i.e

$$\text{tr}_{\mathcal{E}} \left\{ \tilde{H}_I(t_1) \tilde{H}_I(t_2) \cdots \tilde{H}_I(t_{2n+1}) \tilde{\rho}_{\mathcal{E}} \right\} = 0, \quad (1.47)$$

which can also be expressed as

$$\mathcal{P}\mathcal{L}(t_1) \cdots \mathcal{L}(t_{2n+1})\mathcal{P} = 0. \quad (1.48)$$

This assumption is valid for many physical applications. For example in the case of linear coupling between the system and the coordinates of an ensemble of harmonic oscillators the assumption is fulfilled [32]. By applying the projection operators to the Liouville-von Neumann equation (1.39) differential equations for the relevant and irrelevant part are obtained

$$\frac{\partial}{\partial t} \mathcal{P}\tilde{\rho}(t) = \alpha \mathcal{P}\mathcal{L}(t)\tilde{\rho}(t), \quad (1.49)$$

$$\frac{\partial}{\partial t} \mathcal{Q}\tilde{\rho}(t) = \alpha \mathcal{Q}\mathcal{L}(t)\tilde{\rho}(t). \quad (1.50)$$

By inserting the identity $I = \mathcal{P} + \mathcal{Q}$ to (1.50) the differential equations can be

written as

$$\frac{\partial}{\partial t} \mathcal{P}\tilde{\rho}(t) = \alpha \mathcal{P}\mathcal{L}(t) \mathcal{P}\tilde{\rho}(t) + \alpha \mathcal{P}\mathcal{L}(t) \mathcal{Q}\tilde{\rho}(t), \quad (1.51)$$

$$\frac{\partial}{\partial t} \mathcal{Q}\tilde{\rho}(t) = \alpha \mathcal{Q}\mathcal{L}(t) \mathcal{P}\tilde{\rho}(t) + \alpha \mathcal{Q}\mathcal{L}(t) \mathcal{Q}\tilde{\rho}(t). \quad (1.52)$$

The formal solution for (1.52) with initial value $\tilde{\rho}(t_0)$ is

$$\mathcal{Q}\tilde{\rho}(t) = \mathcal{G}(t, t_0) \mathcal{Q}\tilde{\rho}(t_0) + \alpha \int_{t_0}^t ds \mathcal{G}(t, s) \mathcal{Q}\mathcal{L}(s) \tilde{\rho}(s), \quad (1.53)$$

with the propagator $\mathcal{G}(t, s)$ defined as

$$\mathcal{G}(t, s) \equiv I + \sum_{n=1}^{\infty} \alpha^n \int_s^t \int_s^{t_1} \cdots \int_s^{t_{n-1}} \mathcal{Q}\mathcal{L}(t_1) \cdots \mathcal{Q}\mathcal{L}(t_n) dt_n \cdots dt_1. \quad (1.54)$$

Here, the time-ordering is $t \geq t_1 \geq t_2 \geq \cdots \geq t_n \geq \cdots \geq s$. Inserting the formal solution (1.53) into (1.51) one obtains an equation of motion for the relevant part of the density matrix

$$\frac{\partial}{\partial t} \mathcal{P}\tilde{\rho}(t) = \alpha \mathcal{P}\mathcal{L}(t) \mathcal{G}(t, t_0) \mathcal{Q}\tilde{\rho}(t_0) + \alpha \mathcal{P}\mathcal{L}(t) \mathcal{P}\tilde{\rho}(t) + \alpha^2 \int_{t_0}^t ds \mathcal{P}\mathcal{L}(t) \mathcal{G}(t, s) \mathcal{Q}\mathcal{L}(s) \mathcal{P}\tilde{\rho}(s). \quad (1.55)$$

This equation is called the Nakajima-Zwanzig equation. It contains an inhomogeneous term $\alpha \mathcal{P}\mathcal{L}(t) \mathcal{G}(t, t_0) \mathcal{Q}\tilde{\rho}(t_0)$, which depends on the initial condition $\rho(t_0)$. For a factorizing initial condition $\tilde{\rho}(t_0) = \tilde{\rho}_S(t_0) \otimes \tilde{\rho}_E$ one has $\mathcal{Q}\tilde{\rho}(t_0) = 0$ and thus the inhomogeneous term vanishes. The equation has also an integral over the history of the system in the time interval from t_0 to t . This term describes the non-Markovian memory effects of the open system. If the technical assumption (1.47) is made for $n = 0$, i.e. it is assumed that $\tilde{H}_I(t)$ has vanishing diagonal elements with respect to the environment, the term $\alpha \mathcal{P}\mathcal{L}(t) \mathcal{P}\tilde{\rho}(t)$ vanishes and the remaining equation can be written in the form

$$\frac{\partial}{\partial t} \mathcal{P}\tilde{\rho}(t) = \int_{t_0}^t ds \mathcal{K}(t, s) \mathcal{P}\tilde{\rho}(s), \quad (1.56)$$

with the memory kernel

$$\mathcal{K}(t, s) = \alpha^2 \mathcal{P} \mathcal{L}(t) \mathcal{G}(t, s) \mathcal{Q} \mathcal{L}(s) \mathcal{P}. \quad (1.57)$$

This integro-differential equation is exact but might be difficult to solve in many applications. So in next chapter a time-convolutionless form for the master equation is derived.

1.3.2 Time-Convolutionless Projecton Operator Method

The difficulty of solving an integro-differential equation motivates the derivation of a time-convolutionless form of a master equation. The method for removing the time-convolution was developed first in [33]. The idea is simply to replace the density matrix $\tilde{\rho}(s)$ by the solution of equation (1.39). The solution can be written in the form

$$\tilde{\rho}(s) = G(t, s) \tilde{\rho}(t), \quad (1.58)$$

where $G(t, s)$ is called the backward propagator and may be written in the form

$$G(t, s) \equiv I + \sum_{n=1}^{\infty} (-\alpha)^n \int_s^t \int_s^{t_1} \cdots \int_s^{t_n} \mathcal{L}(t_1) \cdots \mathcal{L}(t_n) dt_n \cdots dt_1, \quad (1.59)$$

where the time-ordering is $s \leq t_1 \leq t_2 \leq \cdots \leq t_n \leq \cdots \leq t$. By replacing $\tilde{\rho}(s)$ with the expression $\tilde{\rho}(s) = G(t, s)(\mathcal{P} + \mathcal{Q})\tilde{\rho}(t)$ in the right-hand side of equation (1.53) one obtains

$$\mathcal{Q}\tilde{\rho}(t) = \mathcal{G}(t, t_0) \mathcal{Q}\tilde{\rho}(t_0) + \alpha \int_{t_0}^t ds \mathcal{G}(t, s) \mathcal{Q} \mathcal{L}(s) \mathcal{P} G(t, s) (\mathcal{P} + \mathcal{Q}) \tilde{\rho}(t). \quad (1.60)$$

This can be written in the form

$$[I - \Sigma(t)] \mathcal{Q}\tilde{\rho}(t) = \mathcal{G}(t, t_0) \mathcal{Q}\tilde{\rho}(t_0) + \Sigma(t) \mathcal{P}\tilde{\rho}(t), \quad (1.61)$$

where the super-operator $\Sigma(t)$ is defined as

$$\Sigma(t) \equiv \alpha \int_{t_0}^t ds \mathcal{G}(t, s) \mathcal{Q} \mathcal{L}(s) \mathcal{P} G(t, s). \quad (1.62)$$

The operator $\Sigma(t)$ has the properties $\Sigma(t_0) = 0$ and $\Sigma(t)|_{\alpha=0} = 0$. Thus the operator $[I - \Sigma(t)]$ may be inverted, if the coupling is not too large and for all couplings if $t - t_0$ is small. The irrelevant part for the density matrix, for small couplings or small time-intervals, may be written as

$$\mathcal{Q}\tilde{\rho}(t) = [I - \Sigma(t)]^{-1} \Sigma(t) \mathcal{P}\tilde{\rho}(t) + [I - \Sigma(t)]^{-1} \mathcal{G}(t, t_0) \mathcal{Q}\tilde{\rho}(t_0). \quad (1.63)$$

From this equation it is clear that the irrelevant part of the density matrix $\mathcal{Q}\tilde{\rho}(t)$ depends only on the relevant part $\mathcal{P}\tilde{\rho}(t)$ and on the initial value $\mathcal{Q}\tilde{\rho}(t_0)$ and not on the history of the relevant part as in derivation of the Nakajima-Zwanzig equation. Now to complete the time-convolutionless form of the master equation, (1.63) is inserted into (1.51). The resulting time-convolutionless equation reads

$$\frac{\partial}{\partial t} \mathcal{P}\tilde{\rho}(t) = \mathcal{K}(t)\tilde{\rho}(t) + \mathcal{I}(t)\mathcal{Q}\tilde{\rho}(t_0), \quad (1.64)$$

with the time-convolutionless generator

$$\mathcal{K}(t) \equiv \alpha \mathcal{P}\mathcal{L}(t) [I - \Sigma(t)]^{-1} \mathcal{P} \quad (1.65)$$

and the inhomogeneity

$$\mathcal{I}(t) \equiv \alpha \mathcal{P}\mathcal{L}(t) [I - \Sigma(t)]^{-1} \mathcal{G}(t, t_0) \mathcal{Q}. \quad (1.66)$$

If the factorizing initial condition is assumed, the inhomogeneity vanishes as in the Nakajima-Zwanzig equation. This time-convolutionless form of the master equation is much easier to handle than the integro-differential equation resulting from the Nakajima-Zwanzig equation. But even in the time-convolutionless form the equations of motion may be difficult to solve and a perturbative treatment is then needed in order to achieve a solution for the master equation.

1.3.3 Perturbative Treatment of the Equations

Let us consider the Nakajima-Zwanzig equation with factorizing initial conditions (1.56). The memory kernel can be expanded in the coupling strength α

$$\mathcal{K}(t, s) = \alpha^2 \mathcal{P} \mathcal{L}(t) \mathcal{Q} \mathcal{L}(s) \mathcal{P} + \mathcal{O}(\alpha^3). \quad (1.67)$$

Thus, in second order the integro-differential equation for the relevant part is

$$\frac{\partial}{\partial t} \mathcal{P} \tilde{\rho}(t) = \alpha^2 \int_{t_0}^t ds \mathcal{P} \mathcal{L}(t) \mathcal{L}(s) \mathcal{P} \tilde{\rho}(s). \quad (1.68)$$

When the expressions for the projection operator \mathcal{P} and the Liouvillian $\mathcal{L}(t)$ are inserted one obtains

$$\frac{\partial}{\partial t} \tilde{\rho}_{\mathcal{S}}(t) = -\alpha^2 \int_{t_0}^t d\text{str}_{\mathcal{E}} \left[\tilde{H}_I(t), \left[\tilde{H}_I(s), \tilde{\rho}_{\mathcal{S}}(s) \otimes \tilde{\rho}_{\mathcal{E}} \right] \right]. \quad (1.69)$$

This equation was obtained already in the microscopic derivation before the Markov approximation (1.13).

As noticed in the previous section the generator $\mathcal{K}(t)$ exists only when the operator $[I - \Sigma(t)]$ is invertable. Assume that the operator $[I - \Sigma(t)]$ is such that it may be expanded into a geometric series

$$[I - \Sigma(t)]^{-1} = \sum_{n=0}^{\infty} [\Sigma(t)]^n. \quad (1.70)$$

Now the generator (1.65) can be written as

$$\mathcal{K}(t) = \alpha \sum_{n=0}^{\infty} \mathcal{P} \mathcal{L}(t) [\Sigma(t)]^n \mathcal{P} = \sum_{n=0}^{\infty} \alpha^n \mathcal{K}_n(t). \quad (1.71)$$

To determine $\mathcal{K}_n(t)$ also $\Sigma(t)$ needs to be expanded in powers of α

$$\Sigma(t) = \sum_{n=1}^{\infty} \alpha^n \Sigma_n(t). \quad (1.72)$$

Inserting this into (1.71) one can find for example the second order terms of $\mathcal{K}(t)$:

$$\mathcal{K}_1(t) = \mathcal{P} \mathcal{L}(t) \mathcal{P}, \quad (1.73)$$

$$\mathcal{K}_2(t) = \mathcal{P} \mathcal{L}(t) \Sigma_1(t) \mathcal{P}. \quad (1.74)$$

Making the technical assumption (1.48) again for $n = 0$ it follows that $\mathcal{K}_1(t) = 0$. The first order term $\Sigma_1(t)$ can be calculated from (1.62) by expanding the propagators $\mathcal{G}(t, s)$ and $G(t, s)$ in powers of α . Assuming $t_0 = 0$ the first order term may be written as

$$\Sigma_1(t) = \int_0^t ds \mathcal{Q} \mathcal{L}(s) \mathcal{P}. \quad (1.75)$$

Thus,

$$\mathcal{K}_2(t) = \int_0^t ds \mathcal{P} \mathcal{L}(t) \mathcal{L}(s) \mathcal{P}. \quad (1.76)$$

Writing the projection operator \mathcal{P} and the Liouvillian $\mathcal{L}(t)$ explicitly in (1.76) yields the following equation for the reduced density matrix $\tilde{\rho}_S$,

$$\frac{\partial}{\partial t} \tilde{\rho}_S(t) = -\alpha^2 \int_0^t dstr_{\mathcal{E}} \left[\tilde{H}_I(t), \left[\tilde{H}_I(s), \tilde{\rho}_S(t) \otimes \tilde{\rho}_{\mathcal{E}} \right] \right]. \quad (1.77)$$

This is the same equation which was obtained in the microscopic derivation before the Markov approximation (1.24).

Chapter 2

The Spin-Boson Model

The spin-boson model describes a two-level system interacting with a bosonic environment. The Hamiltonian of the composite system is

$$H = \frac{\epsilon}{2}\sigma_z + \frac{\Delta}{2}\sigma_x + \sum_n \omega_n a_n^\dagger a_n + \frac{\sigma_z}{2} \sum_n \lambda_n (a_n^\dagger + a_n). \quad (2.1)$$

Here,

$$\sigma_z = \begin{pmatrix} 1 & 0 \\ 0 & -1 \end{pmatrix}, \quad \sigma_x = \begin{pmatrix} 0 & 1 \\ 1 & 0 \end{pmatrix} \quad (2.2)$$

in the eigenbasis of the two-state system $\{|e\rangle, |g\rangle\}$, ϵ is the energy bias between the two states, Δ is tunneling amplitude between the states, and ω_n and a_n are the energies and annihilation operators of the corresponding modes of the bosonic environment respectively. The tunneling amplitude Δ is assumed to be a real number. The parameter λ_n describes the coupling strength between the two-state system and the n th mode of the reservoir. The coupling of the system to the environment is a bilinear coupling through operator σ_z , i.e., the environment is sensitive to the value of the operator σ_z . Using the notations of section 1.1 the Hamiltonian can be

divided into three parts:

$$H_S = \frac{\epsilon}{2}\sigma_z + \frac{\Delta}{2}\sigma_x, \quad (2.3)$$

$$H_E = \sum_n \omega_n a_n^\dagger a_n, \quad (2.4)$$

$$H_I = \frac{\sigma_z}{2} \sum_n \lambda_n (a_n^\dagger + a_n). \quad (2.5)$$

In this section the Hamiltonian is considered without any specific physical context. Thus the parameter space is not restricted by any means. In section 4 some physical applications for the spin-boson model are presented. The approximations performed in the derivation of the master equation are not justified in all the possible physical applications presented, but nonetheless the relatively simple mathematical description obtained, when the approximations are justified makes the interpretation of the physical features of the system more straightforward.

2.1 Derivation of the Master Equation

The aim is to derive a time-convolutionless master equation describing the reduced dynamics of the system under the Hamiltonian (2.1). The starting point of the derivation is the general form of the second order time-convolutionless master equation (1.77). This description corresponds to the one presented in the microscopic derivation (1.24) with the expansion parameter α embedded into the interaction Hamiltonian. In the case of a bosonic reservoir the technical assumption (1.47) in the derivation of the time-convolutionless master equation is no longer an assumption, because the term assumed to be zero actually vanishes completely. In summary, the second order time-convolutionless master equation can be written in the form

$$\frac{d}{dt}\tilde{\rho}_S(t) = - \int_0^t \text{tr}_E[\tilde{H}_I(t), [\tilde{H}_I(t'), \tilde{\rho}_S(t) \otimes \rho_E]]dt'. \quad (2.6)$$

To obtain a physically intuitive description of the dynamics it is convenient to perform the secular approximation. This is easy once the master equation (2.6) is

written in terms of the system eigenoperators.

2.1.1 Calculation of the Eigenoperators

The interaction Hamiltonian can be written as a decomposition of the system eigenoperators defined in (1.32). To obtain this decomposition, the system eigenvalues and the corresponding eigenoperators need to be calculated. The system eigenvalues are

$$\lambda_+ = \frac{1}{2}\sqrt{\epsilon^2 + \Delta^2}, \quad \lambda_- = -\frac{1}{2}\sqrt{\epsilon^2 + \Delta^2} \quad (2.7)$$

and the corresponding eigenvectors

$$|\psi_+\rangle = \frac{\Delta|e\rangle + (\omega_0 - \epsilon)|g\rangle}{\sqrt{2\omega_0(\omega_0 - \epsilon)}}, \quad |\psi_-\rangle = \frac{-\Delta|e\rangle + (\omega_0 + \epsilon)|g\rangle}{\sqrt{2\omega_0(\omega_0 + \epsilon)}}, \quad (2.8)$$

where $\omega_0 = \sqrt{\epsilon^2 + \Delta^2}$. The system eigenoperators are obtained using equation (1.32). In the system eigenbasis $\{|\psi_+\rangle, |\psi_-\rangle\}$ the system eigenoperators may be written in the following simple form,

$$S(0) = \frac{\epsilon}{2\omega_0}\sigma_z, \quad S(\omega_0) = -\frac{\Delta}{2\omega_0}\sigma_-, \quad S(-\omega_0) = -\frac{\Delta}{2\omega_0}\sigma_+. \quad (2.9)$$

Here,

$$\sigma_z = \begin{pmatrix} 1 & 0 \\ 0 & -1 \end{pmatrix}, \quad \sigma_+ = \begin{pmatrix} 0 & 1 \\ 0 & 0 \end{pmatrix}, \quad \sigma_- = \begin{pmatrix} 0 & 0 \\ 1 & 0 \end{pmatrix}, \quad (2.10)$$

in the system eigenbasis $\{|\psi_+\rangle, |\psi_-\rangle\}$. The system eigenbasis is a proper choice for studying thermalization process [13] and it is also the so called preferred basis in studying the decoherence process in the weak coupling limit. The concept of preferred basis will be discussed in chapter 2.3.1. If the secular approximation is performed, the dynamics of the reduced system is described by equation (1.35).

Now the form of the master equation is known, but the explicit expression for the time dependent coefficients

$$\Gamma_\omega(t) \equiv \int_0^t dt' e^{i\omega t'} \text{tr}_\mathcal{E} \left\{ \tilde{E}^\dagger(t) \tilde{E}(t-t') \rho_\mathcal{E} \right\} = \int_0^t dt' e^{i\omega t'} \text{tr}_\mathcal{E} \left\{ \tilde{E}^\dagger(t') \tilde{E}(0) \rho_\mathcal{E} \right\} \quad (2.11)$$

in the master equation is unknown. There is not yet enough information about the system to determine these coefficients. Each of the modes of the reservoir couple to the system with different strength. To fully determine the dynamics it must be known how the coupling strength is distributed.

2.1.2 Determining the Decay Rates

The master equation for the spin-boson model is of the form

$$\dot{\tilde{\rho}}_S(t) = -i[H_{LS}(t), \tilde{\rho}_S(t)] + \mathcal{D}(t)(\tilde{\rho}_S(t)), \quad (2.12)$$

with

$$\mathcal{D}(t)(\tilde{\rho}_S(t)) = \sum_{\omega} \gamma_{\omega}(t) \left[S(\omega) \tilde{\rho}_S(t) S^{\dagger}(\omega) - \frac{1}{2} \{ S^{\dagger}(\omega) S(\omega), \tilde{\rho}_S(t) \} \right]. \quad (2.13)$$

and

$$H_{LS}(t) = \sum_{\omega} \lambda_{\omega}(t) S^{\dagger}(\omega) S(\omega). \quad (2.14)$$

The time-dependent coefficients $\gamma_{\omega}(t)$ and $\lambda_{\omega}(t)$ in (2.13) and (2.14) are the real and imaginary parts of (2.11) respectively.

It is convenient at this point to assume that the bosonic environment is thermal. This enables one to calculate the expression $\text{tr}_{\mathcal{E}} \{ \tilde{E}^{\dagger}(t') \tilde{E}(0) \rho_{\mathcal{E}} \}$ in the coefficient (2.11). The expression can be written in the form

$$\begin{aligned} \text{tr}_{\mathcal{E}} \{ \tilde{E}^{\dagger}(t') \tilde{E}(0) \rho_{\mathcal{E}} \} &= \sum_{k,l} \lambda_k \lambda_l \text{tr}_{\mathcal{E}} \{ (a_k^{\dagger}(t') + a_k(t')) (a_l^{\dagger} + a_l) \rho_{\mathcal{E}} \} \\ &= \sum_{k,l} \lambda_k \lambda_l \left[\text{tr}_{\mathcal{E}} \{ a_k^{\dagger}(t') a_l^{\dagger} \tilde{\rho}_{\mathcal{E}} \} + \text{tr}_{\mathcal{E}} \{ a_k^{\dagger}(t') a_l \tilde{\rho}_{\mathcal{E}} \} \right. \\ &\quad \left. + \text{tr}_{\mathcal{E}} \{ a_k(t') a_l^{\dagger} \tilde{\rho}_{\mathcal{E}} \} + \text{tr}_{\mathcal{E}} \{ a_k(t') a_l \tilde{\rho}_{\mathcal{E}} \} \right]. \end{aligned} \quad (2.15)$$

Here, the bosonic creation and annihilation operators in the interaction picture are

$$a_k(t) = e^{-i\omega_k t} a_k \quad \text{and} \quad a_k^{\dagger}(t) = e^{i\omega_k t} a_k^{\dagger}. \quad (2.16)$$

The partial traces in expression (2.16) can be calculated for a thermal reservoir [34]

$$\begin{aligned}
\mathrm{tr}_{\mathcal{E}} \left\{ a_k^\dagger(t') a_l^\dagger \tilde{\rho}_{\mathcal{E}} \right\} &= e^{i\omega_k t'} \mathrm{tr}_{\mathcal{E}} \left\{ b_k^\dagger b_l^\dagger \tilde{\rho}_{\mathcal{E}} \right\} = 0, \\
\mathrm{tr}_{\mathcal{E}} \left\{ a_k^\dagger(t') a_l \tilde{\rho}_{\mathcal{E}} \right\} &= e^{i\omega_k t'} \mathrm{tr}_{\mathcal{E}} \left\{ b_k^\dagger b_l \tilde{\rho}_{\mathcal{E}} \right\} = e^{i\omega_k t'} \delta_{kl} N(\omega_k), \\
\mathrm{tr}_{\mathcal{E}} \left\{ a_k(t') a_l^\dagger \tilde{\rho}_{\mathcal{E}} \right\} &= e^{-i\omega_k t'} \mathrm{tr}_{\mathcal{E}} \left\{ b_k b_l^\dagger \tilde{\rho}_{\mathcal{E}} \right\} = e^{-i\omega_k t'} \delta_{kl} (N(\omega_k) + 1), \\
\mathrm{tr}_{\mathcal{E}} \left\{ a_k(t') a_l \tilde{\rho}_{\mathcal{E}} \right\} &= e^{-i\omega_k t'} \mathrm{tr}_{\mathcal{E}} \left\{ b_k b_l \tilde{\rho}_{\mathcal{E}} \right\} = 0.
\end{aligned} \tag{2.17}$$

Here, $N(\omega_k)$ is the Bose-Einstein distribution

$$N(\omega_k) = (e^{\omega_k/T} - 1)^{-1}, \tag{2.18}$$

where we have put $k_B = 1$.

A system can often be described as a two-state system if the temperature is sufficiently small. Thus, most applications of the spin-boson model are systems at low temperatures. This fact makes it reasonable to study the model with temperature $T \simeq 0$. In zero temperature all the modes in the bosonic environment are in the ground state and the Bose-Einstein distribution, describing the number of excitations of the reservoir oscillator having frequency ω , is zero for all k . The coefficient $\Gamma_\omega(t)$ is of the form

$$\begin{aligned}
\Gamma_\omega(t) &= \int_0^t dt' \sum_k \lambda_k^2 (N(\omega_k) e^{i(\omega+\omega_k)t'} + (N(\omega_k) + 1) e^{i(\omega-\omega_k)t'}) \\
&\xrightarrow{T \rightarrow 0} \int_0^t dt' \sum_k \lambda_k^2 e^{i(\omega-\omega_k)t'}.
\end{aligned} \tag{2.19}$$

Because the frequencies of the reservoir oscillators $\{\omega_k | k \in \mathbb{N}\}$ are dense in the parameter space one can go to continuum limit ($\sum_k \lambda_k^2 \rightarrow \int_0^\infty d\omega' J(\omega')$) and write $\Gamma_\omega(t)$ in the form

$$\Gamma_\omega(t) = \int_0^t dt' \int_0^\infty d\omega' J(\omega') e^{i(\omega-\omega')t'}. \tag{2.20}$$

Here, the function $J(\omega)$ describes how the strength of the coupling between the system and the environment is distributed.

In the master equation (2.12) there appears the real and imaginary parts of $\Gamma_\omega(t)$. The real part appearing in the dissipator (2.13) is

$$\gamma_\omega(t) = 2\Re[\Gamma_\omega(t)] = 2 \int_0^t dt' \int_0^\infty d\omega' J(\omega') \cos(\omega - \omega')t' \quad (2.21)$$

and the imaginary part in the Lamb shift Hamiltonian (2.14) is

$$\lambda_\omega(t) = \Im[\Gamma_\omega(t)] = \int_0^t dt' \int_0^\infty d\omega' J(\omega') \sin(\omega - \omega')t'. \quad (2.22)$$

The master equation (2.12) can be interpreted as describing changes in the system through reaction channels with a certain reaction described by the operator $S(\omega)$ and the rate of the reaction by $\gamma_\omega(t)$. Because the system is decaying due to the interaction with the environment the rates $\gamma_\omega(t)$ are generally known as decay rates.

The master equation (2.12) in the interaction picture consists of two parts: the dissipator and the Lamb shift. In the Schrödinger picture the master equation is obtained only by adding the system Hamiltonian to the Lamb shift Hamiltonian. Thus,

$$\dot{\rho}_S(t) = -i[H_S + H_{LS}(t), \rho_S(t)] + \mathcal{D}(t)(\rho_S(t)). \quad (2.23)$$

In the system eigenbasis $\{|\psi_+\rangle, |\psi_-\rangle\}$ the system Hamiltonian is the diagonal matrix $\frac{\omega_0}{2}\sigma_z$. In this basis the first term in equation (2.23) can be written in the form

$$\begin{aligned} [H_S + H_{LS}(t), \rho_S(t)] &= \left[\frac{\omega_0}{2}\sigma_z + H_{LS}(t), \rho_S(t) \right] \\ &= \left[\frac{\omega_0 + \frac{\Delta^2}{4\omega_0^2}(\lambda_{\omega_0}(t) - \lambda_{\omega_0}(t))}{2}\sigma_z, \rho_S(t) \right] \\ &= \left[\frac{\omega_0 + E_{LS}(t)}{2}\sigma_z, \rho_S(t) \right]. \end{aligned} \quad (2.24)$$

What can be seen from this expression is that the Lamb shift Hamiltonian only shifts the system eigenenergies due to the interaction with the environment and does not really contribute to the qualitative behavior of the system. Thus the Lamb shift

Hamiltonian is ignored throughout this thesis and the center of focus will be laid on the dissipator (2.13) and thereby the time-dependent decay rates $\gamma_\omega(t)$.

To calculate the decay rates (2.21), one needs to specify the spectral function $J(\omega)$. The form of the spectral function depends on the specific application of the model, but the characteristic nature of the system can be described with a simple Ohmic function

$$J(\omega) = \frac{\alpha}{2} \omega e^{-\frac{\omega}{\omega_c}}, \quad (2.25)$$

in which α is a coupling constant and ω_c is the cutoff frequency. Here, an exponential cutoff is used. The arbitrary choice of the cutoff does not change the structure of the reservoir and thus the Lorentz-Drude cutoff, used e.g. in [1], would yield the same dynamics. With this spectral function the integrals in (2.21) can be calculated and the explicit form of the obtained decay rates is

$$\begin{aligned} \gamma_{\pm\omega_0}(t) &= \frac{\alpha\omega_c}{1 + \omega_c^2 t^2} [\omega_c t \cos(\omega_0 t) \mp \sin(\omega_0 t)] \\ &+ \alpha\omega_0 e^{\mp\omega_0/\omega_c} \left[\Re \left[\text{Si}(\omega_0 t + i\frac{\omega_0}{\omega_c}) \right] \mp \Im \left[\text{Ci}(\omega_0 t + i\frac{\omega_0}{\omega_c}) \right] \pm \frac{\pi}{2} \right] \\ \gamma_0(t) &= \frac{\alpha\omega_c^2 t}{1 + \omega_c^2 t^2}, \end{aligned} \quad (2.26)$$

where $\text{Ci}(z)$ is the cosine integral and $\text{Si}(z)$ is the sine integral. The decay rates are plotted in figure 2.1 In summary, the form of the relevant equation of motion for the reduced density matrix is

$$\dot{\rho}_S(t) = -i[H_S, \rho_S(t)] + \mathcal{D}(t)(\rho_S(t)), \quad (2.27)$$

where

$$H_S = \frac{\omega_0}{2} \sigma_z \quad (2.28)$$

and

$$\mathcal{D}(t)(\rho_S(t)) = \sum_{\omega} \gamma_{\omega}(t) \left[S(\omega) \rho_S(t) S^\dagger(\omega) - \frac{1}{2} \{ S^\dagger(\omega) S(\omega), \rho_S(t) \} \right] \quad (2.29)$$

with the eigenoperators

$$S(0) = \frac{\epsilon}{2\omega_0}\sigma_z, \quad S(\omega_0) = -\frac{\Delta}{2\omega_0}\sigma_-, \quad S(-\omega_0) = -\frac{\Delta}{2\omega_0}\sigma_+. \quad (2.30)$$

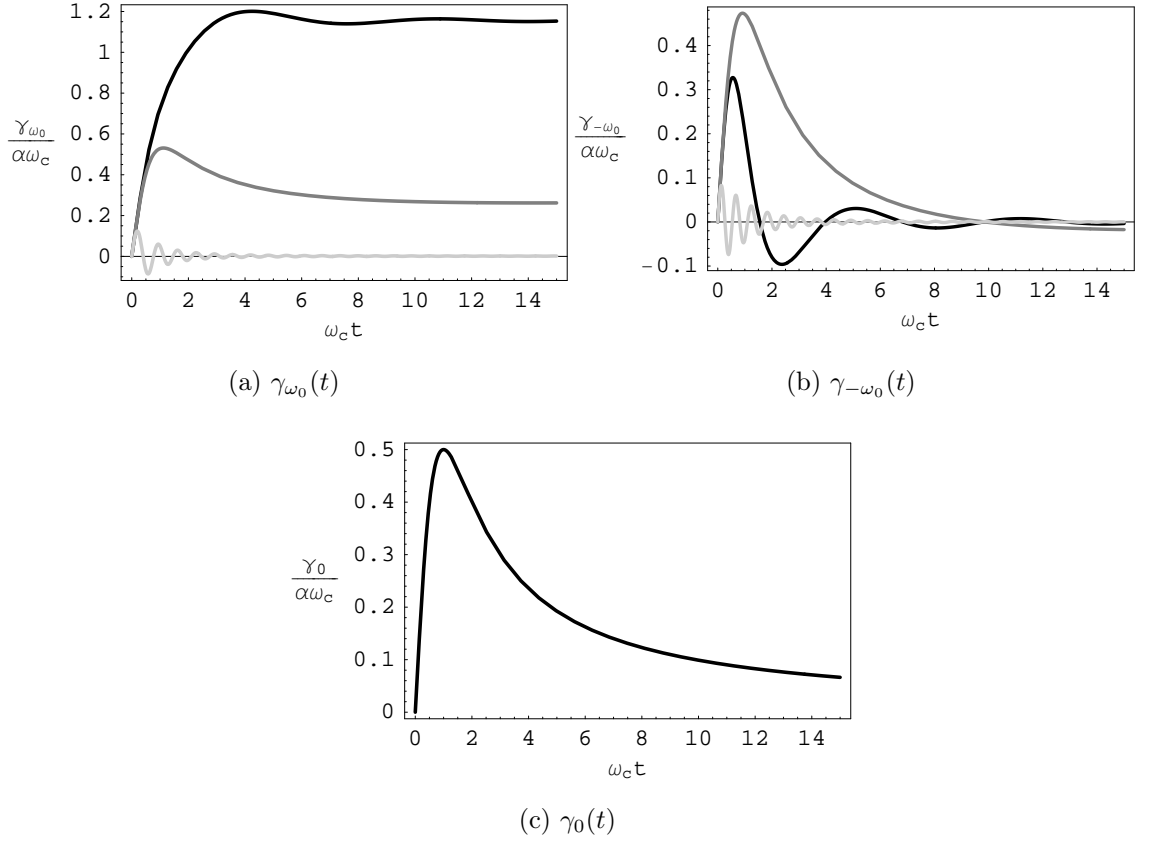


Figure 2.1: The evolution of the decay rates $\gamma_{\omega_0}(t)$, $\gamma_{-\omega_0}(t)$ and $\gamma_0(t)$ with respect to $\omega_c t$ for the values $\frac{\omega_0}{\omega_c} = 1$ (black line), $\frac{\omega_0}{\omega_c} = 0.1$ (dark gray line) and $\frac{\omega_0}{\omega_c} = 10$ (light gray line). In (c) it can be seen that the decay rate $\gamma_0(t)$ is the same for all values of $\frac{\omega_0}{\omega_c}$.

The equations of motion for the matrix elements of the reduced density matrix

in the interaction picture resulting from (2.27) are

$$\begin{cases} \dot{\rho}_{++}(t) &= \frac{\Delta^2}{4\omega_0^2} \left[\gamma_{-\omega_0}(t) - (\gamma_{\omega_0}(t) + \gamma_{-\omega_0}(t))\rho_{++}(t) \right], \\ \Re[\dot{\rho}_{+-}(t)] &= -\frac{4\epsilon^2\gamma_0(t) + \Delta^2(\gamma_{\omega_0}(t) + \gamma_{-\omega_0}(t))}{8\omega_0^2} \Re[\rho_{+-}(t)], \\ \Im[\dot{\rho}_{+-}(t)] &= -\frac{4\epsilon^2\gamma_0(t) + \Delta^2(\gamma_{\omega_0}(t) + \gamma_{-\omega_0}(t))}{8\omega_0^2} \Im[\rho_{+-}(t)]. \end{cases} \quad (2.31)$$

The solution of this differential equation can be written in the following form:

$$\rho(t) = \begin{pmatrix} e^{-\eta(t)}(\xi(t) + 1) & 0 & 0 & e^{-\eta(t)}\xi(t) \\ 0 & e^{-\zeta(t)} & 0 & 0 \\ 0 & 0 & e^{-\zeta(t)} & 0 \\ 1 - e^{-\eta(t)}(\xi(t) + 1) & 0 & 0 & 1 - e^{-\eta(t)}\xi(t) \end{pmatrix} \rho(0). \quad (2.32)$$

Here,

$$\eta(t) = \frac{\Delta^2}{4\omega_0^2} \int (\gamma_{\omega_0}(t) + \gamma_{-\omega_0}(t)) dt, \quad (2.33)$$

$$\xi(t) = \frac{\Delta^2}{4\omega_0^2} \int \gamma_{-\omega_0} e^{-\eta(t)} dt, \quad (2.34)$$

$$\zeta(t) = \int \left(\frac{\epsilon^2}{2\omega_0^2} \gamma_0(t) + \frac{\Delta^2}{8\omega_0^2} (\gamma_{\omega_0}(t) + \gamma_{-\omega_0}(t)) \right) dt. \quad (2.35)$$

The matrix in equation (2.32) acts on $\rho(0)$ as on a column vector consisting of the density matrix elements.

2.2 Numerical Solution to the Master Equation

The master equation (2.27) can be solved numerically and in this section some numerical results for different parameter values are presented. All the plots presented in this section are for the initial state $|\psi(0)\rangle = \frac{1}{\sqrt{2}}(|\psi_+\rangle + |\psi_-\rangle)$.

When the parameters are chosen such that $\omega_0 \ll \omega_c$, the bath correlation time τ_c is much smaller than the typical time scale of the system τ_s and the environmental memory does not affect the system dynamics. The decay rates settle into their

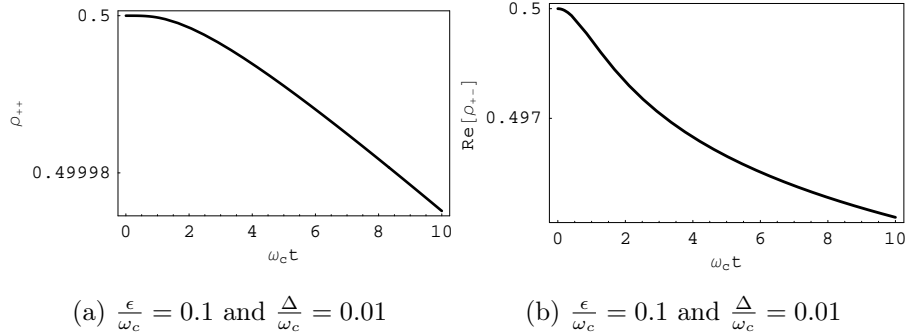


Figure 2.2: The population of state $|\psi_+\rangle$ ρ_{++} (a) and coherence $\Re[\rho_{+-}]$ (b) for different parameter values in the case of a flat reservoir spectrum, i.e. $\frac{\omega_0}{\omega_c} \ll 1$. Here, the coupling constant is $\alpha = 0.01$.

Markovian values very fast and thus the non-Markovian master equation gives the same dynamics as the Markovian master equation. The system dynamics with such parameter values is plotted in figure 2.2.

When $\omega_0 \gg \omega_c$, the bath correlation time is larger than the typical time scale of the system, which results in strong memory effects in the system dynamics. In this case the decay rates are oscillating and they get temporarily negative values. These negative regions lead to oscillatory behavior in the populations and coherences as can be seen in figure 2.3. This oscillatory behavior and the meaning of the negative values of the decay rates is studied more profoundly in section 3 where the master equation is unraveled in terms of individual wave function realizations.

For fixed ω_0 and ω_c the memory time of the environment is also fixed and it is not dependent on the proportion of ϵ and Δ . It can be seen in figures 2.3d and 2.3f that as ϵ becomes larger than Δ the recoherence effect visible in figure 2.3b is destroyed and the decoherence process becomes faster. The recoherence process is studied in more detail in section 3.3.

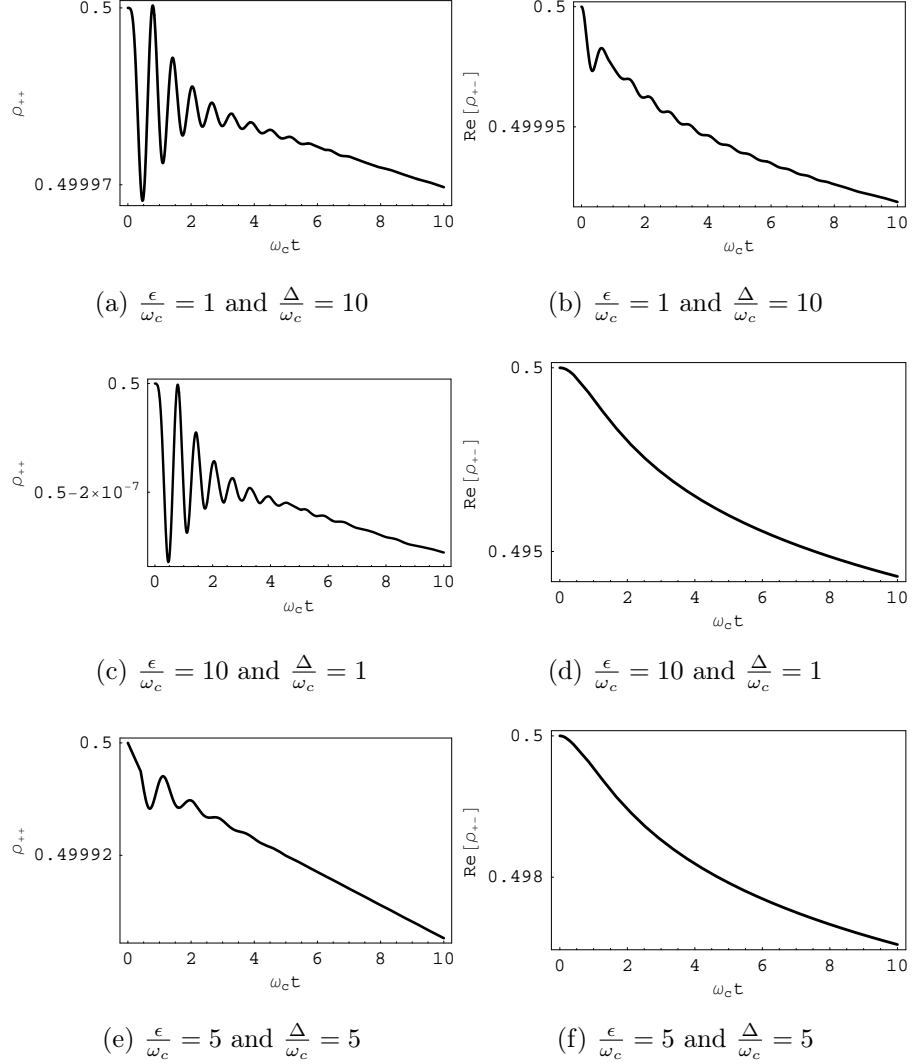


Figure 2.3: The population of state $|\psi_+\rangle$ ρ_{++} [(a), (c) and (e)] and coherence $\Re[\rho_{+-}]$ [(b), (d) and (f)] for different parameter values in the case of a structured reservoir, i.e. $\frac{\omega_0}{\omega_c} \gg 1$. Here, the coupling constant is $\alpha = 0.01$.

2.3 Special Cases

To distinguish the different physical processes affecting the system dynamics and to compare the results of this thesis with earlier results on the spin-boson model it is

convenient to study the dynamics without tunneling ($\Delta = 0$) or without energy bias ($\epsilon = 0$). It is also important to study the Markovian case to find out what kind of effects non-Markovianity actually has on the dynamics and to determine the time scale of relaxation in the system.

2.3.1 Limit of Pure Dephasing, No Tunneling

The Hamiltonian (2.1) without the tunneling element $\frac{\Delta}{2}\sigma_x$ reads

$$H = \frac{\epsilon}{2}\sigma_z + \sum_n \omega_n a_n^\dagger a_n + \frac{\sigma_z}{2} \sum_n \lambda_n (a_n^\dagger + a_n). \quad (2.36)$$

In this case the system Hamiltonian commutes with the interaction Hamiltonian, $[H_S, H_I] = 0$, and thus there is no energy exchange between the system and the environment. The process induced by the Hamiltonian (2.36) is called dephasing of qubits and it has been studied extensively due to its role in the measurement problem [35] and in the context of quantum computers [36]. The term dephasing is used for a process in which the off-diagonal elements of the density matrix get reduced in the energy eigenstate of the system. So the term is used for an effect and not for the cause. In the next section decoherence, the process behind dephasing in some cases, is studied in more detail.

Decoherence

The study of decoherence has been of great interest during the last few decades not only due to its relevance in the field of quantum information processing, but also for its role in the emergence of classicality within quantum mechanical description of the world [37]. Before the concept of decoherence was introduced as a possible elucidator of the border between the classical and quantum descriptions, the mainstream attitude was that the problem was purely philosophical and could not be solved by physical analysis. Throughout this thesis we use the term decoherence for the

environment induced and purely quantum mechanical decaying of the off-diagonal elements of the density matrix.

Decoherence is a consequence of quantum entanglement between the system and the environment. The process describes the destruction of some superposed states due to quantum mechanical effects. But not all quantum superpositions are treated equally by decoherence. The interaction typically singles out a preferred set of states which are not influenced by decoherence. These pointer states [35] remain unchanged in spite of the environment but their superpositions decohere. This decoherence-imposed selection of the preferred set of pointer states is called environment-induced superselection.

The sensitivity of a particular state is determined by the structure of the interaction. The strength of the interaction determines the choice for the preferred states. In the case of weak interaction the system Hamiltonian H_S dominates the evolution and pointer states will arise that are the energy eigenstates of H_S [38].

Solution to the Master Equation

In the case of no tunneling in the system we set $\Delta = 0$ and the master equation (2.27) becomes very simple. The eigenoperators (2.30) are

$$S(0) = \frac{1}{2}\sigma_z, \quad S(\omega_0) = S(-\omega_0) = 0 \quad (2.37)$$

and the dissipator is simply

$$\mathcal{D}(t)(\rho_S(t)) = \gamma_0(t) \left[S(0)\rho_S(t)S^\dagger(0) - \frac{1}{2} \{S^\dagger(0)S(0), \rho_S(t)\} \right]. \quad (2.38)$$

The equations of motion for the elements of the reduced density matrix in the interaction picture are

$$\dot{\rho}_{S00} = 0, \quad \dot{\rho}_{S01} = -\frac{\gamma_0(t)}{2}\rho_{S01}. \quad (2.39)$$

Thus, the populations are unchanged and the off-diagonal elements decay exponentially. Inserting the decay rate $\gamma_0(t)$ (2.26) yields the following expression for the off-diagonal elements of the reduced density matrix:

$$\rho_{\mathcal{S}_{01}}(t) = \rho_{\mathcal{S}_{01}}(0)(1 + \omega_c^2 t^2)^{-\alpha/4}. \quad (2.40)$$

The decoherence time, i.e. the decay time of the off-diagonal elements, is

$$\tau_{\text{decoh}} = \frac{(e^{4/\alpha} - 1)^{1/2}}{\omega_c}. \quad (2.41)$$

With non-zero but low ($T \ll \omega_c$) temperature the off-diagonal density matrix is [36]

$$\rho_{\mathcal{S}_{01}}(t) = \rho_{\mathcal{S}_{01}}(0)(1 + \omega_c^2 t^2)^{-\alpha/4} \left(\frac{\sinh(\pi T t)}{\pi T t} \right)^{-\alpha/2}. \quad (2.42)$$

Here, the term $\left(\frac{\sinh(\pi T t)}{\pi T t} \right)^{-\alpha/2}$ describes the effect of thermal fluctuations on dephasing. In the limit $T \rightarrow 0$ the expression reduces to (2.40).

The quantum vacuum fluctuations, i.e. the decoherence produced by the interaction with the environment, will contribute to the dephasing process only for times $t > \omega_c^{-1}$ [36]. There are three different regimes for the decoherence :

- a 'quiet' regime, for $t < \omega_c^{-1}$, where the coherence is unaffected by the fluctuations;
- a quantum regime, for $\omega_c^{-1} < t < T^{-1}$, where the main cause of decoherence are the quantum vacuum fluctuations;
- a thermal regime, for $t > T^{-1}$, where thermal fluctuations play the major role in decoherence.

The three different time regimes for decoherence are demonstrated in figure 2.4. One can see that the quantum fluctuations originate from the non-Markovian character of the decay rate $\gamma_0(t)$. If the Markov approximation was performed, the decoherence

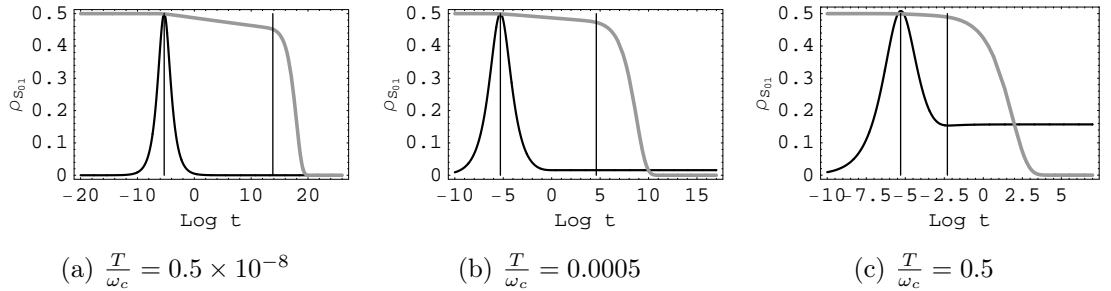


Figure 2.4: The non-diagonal element $\rho_{S_{01}}$ of the system density matrix (gray line) and the scaled decay rate $\gamma_0(t)$ (black line) with the initial value $\rho_{S_{01}}(0) = 0.5$ and $\alpha = 0.01$. The vertical lines represent the times $t = \frac{1}{\omega_c}$ and $t = \frac{1}{T}$.

would arise only from thermal fluctuations. Thus in the zero temperature case, where the stationary value of $\gamma_0(t)$ is zero, there would be no dephasing. This would not be a satisfactory description of the dynamics and therefore the non-Markovian description is necessary.

2.3.2 Tunneling Dynamics, Zero Energy Bias

One can simplify the Hamiltonian (2.1) by putting the energy bias $\epsilon = 0$. Hamiltonian of this form has been studied for example in [1]. It can be written in the system eigenbasis as

$$H = \frac{\Delta}{2}\sigma_z + \sum_n \omega_n a_n^\dagger a_n - \frac{\sigma_x}{2} \sum_n \lambda_n (a_n^\dagger + a_n). \quad (2.43)$$

Using the second order time convolutionless projection operator method, the following master equation for the Bloch vector $\langle \vec{\sigma}(t) \rangle$ is gained in [1]

$$\frac{d}{dt} \langle \vec{\sigma}(t) \rangle = A(t) \langle \vec{\sigma}(t) \rangle + 2\vec{b}(t), \quad (2.44)$$

where the Bloch vector is

$$\langle \vec{\sigma}(t) \rangle = \text{tr} \{ \vec{\sigma} \rho_S(t) \} \quad (2.45)$$

with

$$\vec{\sigma} = (\sigma_x, \sigma_y, \sigma_z)^T \quad (2.46)$$

and

$$A(t) = \begin{pmatrix} 0 & -\Delta & 0 \\ \Delta - 2E_{LS}(t) & -\frac{\gamma_{\omega_0}(t) + \gamma_{-\omega_0}(t)}{4} & 0 \\ 0 & 0 & -\frac{\gamma_{\omega_0}(t) + \gamma_{-\omega_0}(t)}{4} \end{pmatrix},$$

$$\vec{b}(t) = \begin{pmatrix} 0 \\ 0 \\ -\frac{1}{8}(\gamma_{\omega_0} - \gamma_{-\omega_0}) \end{pmatrix}. \quad (2.47)$$

Here, $E_{LS}(t) = \frac{1}{4}[\lambda_{-\omega_0}(t) - \lambda_{\omega_0}(t)]$ and the factors $\gamma_{\pm\omega_0}(t)$ are the ones in equation (2.26) with $\omega_0 = \Delta$, and $\lambda_{\pm\omega_0}(t)$ can be calculated from (2.22). In this form of the master equation no secular approximation is performed and thus the result differs from the master equation derived in chapter 2.1.2. To ensure the validity of the secular approximation it should be checked in which parts of the parameter space the two master equations coincide.

When $\epsilon = 0$ in the Hamiltonian (2.1) the eigenoperators (2.9) are

$$S(0) = 0, \quad S(\omega_0) = -\frac{1}{2}\sigma_-, \quad S(-\omega_0) = -\frac{1}{2}\sigma_+. \quad (2.48)$$

By inserting these operators into the master equation (2.12), in which the secular approximation is performed, the consequent equation for the Bloch vector (2.45) reads

$$\frac{d}{dt} \langle \vec{\sigma}(t) \rangle = A(t) \langle \vec{\sigma}(t) \rangle + 2\vec{b}(t), \quad (2.49)$$

where

$$\begin{aligned}
A(t) &= \begin{pmatrix} -\frac{1}{8}(\gamma_{\omega_0}(t) + \gamma_{-\omega_0}(t)) & -\Delta & 0 \\ \Delta & -\frac{1}{8}(\gamma_{\omega_0}(t) + \gamma_{-\omega_0}(t)) & 0 \\ 0 & 0 & -\frac{1}{4}(\gamma_{\omega_0}(t) + \gamma_{-\omega_0}(t)) \end{pmatrix}, \\
\vec{b}(t) &= \begin{pmatrix} 0 \\ 0 \\ -\frac{1}{8}(\gamma_{\omega_0} - \gamma_{-\omega_0}) \end{pmatrix}. \tag{2.50}
\end{aligned}$$

The vectors $\vec{b}(t)$ in (2.47) and (2.50) coincide, but the matrices $A(t)$ differ for some regions of the parameter space.

When deriving the master equation (2.27) for the spin-boson model, the Lamb shift Hamiltonian (2.14) was ignored because of its lack of influence on the qualitative behavior of the system. The energy shift $E_{LS}(t)$ which was ignored previously arises also in the matrix (2.47). For consistency, the Lamb shift energy will be left out also from the matrix (2.47).

The differences in the dynamics presented by the matrices (2.47) and (2.50) can be studied by writing the second order differential equations for the Bloch vector component $\langle \sigma_x(t) \rangle$ in the presence and absence of the secular approximation. By comparing the resulting second order differential equations one obtains the following condition for the validity of the secular approximation:

$$\frac{1}{4} [\gamma_{\omega_0}(t) + \gamma_{-\omega_0}(t)]^2 + \frac{1}{2} \frac{d}{dt} [\gamma_{\omega_0}(t) + \gamma_{-\omega_0}(t)] \ll \Delta^2 \quad \Rightarrow \quad \frac{\Delta}{\omega_c} \gg \alpha. \tag{2.51}$$

More general conditions for the validity of the secular approximation will be derived in section 2.4 by studying different time scales appearing in the dynamics. It will be seen that the validity of those general conditions also imply the condition (2.51).

2.3.3 Markovian Case

To actually know what kind of effects the non-Markovianity has on the dynamics the Markovian case needs to be unraveled first. To gain a more general expression the Markovian case is studied with non-zero temperature. The form of the master equation is the same in the Markovian and the non-Markovian case but the decay rates in (2.27) do not depend on time in the Markovian case. The decay rates can be calculated by using (2.19) and putting $t \rightarrow \infty$.

$$\begin{aligned}
\gamma_\omega(t) &= \Gamma_\omega(t) + \Gamma_\omega^*(t) \\
&= 2 \int_0^t dt' \int_0^\infty d\omega' J(\omega') [N(\omega') \cos((\omega' + \omega)t') + (N(\omega') + 1) \cos((\omega' - \omega)t')] \\
&= 2 \int_0^\infty d\omega' J(\omega') \left[N(\omega') \frac{\sin((\omega' + \omega)t)}{\omega' + \omega} + (N(\omega') + 1) \frac{\sin((\omega' - \omega)t)}{\omega' - \omega} \right]. \quad (2.52)
\end{aligned}$$

By putting $t \rightarrow \infty$ and using the formal expression

$$\lim_{t \rightarrow \infty} \frac{\sin((\omega' + \omega)t)}{\omega' + \omega} = \pi \delta(\omega' + \omega) \quad (2.53)$$

the Markovian decay rates can be written as

$$\begin{aligned}
\gamma_{\omega_0} &= 2\pi J(\omega_0)(N(\omega_0) + 1), \\
\gamma_{-\omega_0} &= 2\pi J(\omega_0)N(\omega_0), \\
\gamma_0 &= 0. \quad (2.54)
\end{aligned}$$

Once the decay rates are known one can write the differential equations for the density matrix elements from the master equation (1.35). They have the well known Bloch equation form in the system eigenbasis:

$$\begin{aligned}
\dot{\rho}_{++} &= \frac{\Delta^2}{4\omega_0^2} [\gamma_{\omega_0} - (\gamma_{\omega_0} + \gamma_{-\omega_0})\rho_{++}], \\
\Re[\dot{\rho}_{+-}] &= \frac{1}{8\omega_0^2} [-8\omega_0^3 \Im[\rho_{+-}] - \Delta^2(\gamma_{\omega_0} + \gamma_{-\omega_0})\Re[\rho_{+-}]], \\
\Im[\dot{\rho}_{+-}] &= \frac{1}{8\omega_0^2} [-\Delta^2(\gamma_{\omega_0} + \gamma_{-\omega_0})\Im[\rho_{+-}] + 8\omega_0^3 \Re[\rho_{+-}]]. \quad (2.55)
\end{aligned}$$

This group of differential equations can be solved analytically. The eigenstate probability and the coherences are

$$\begin{aligned}\rho_{++}(t) &= \frac{\gamma_{-\omega_0} + \exp[-\frac{\Delta^2}{\omega_0^2}(\gamma_{\omega_0} + \gamma_{-\omega_0})t](\rho_{++}(0)(\gamma_{\omega_0} + \gamma_{-\omega_0}) - \gamma_{-\omega_0})}{\gamma_{\omega_0} + \gamma_{-\omega_0}}, \quad (2.56) \\ \Re[\rho_{+-}(t)] &= \exp[-\frac{\Delta^2}{2\omega_0^2}(\gamma_{\omega_0} + \gamma_{-\omega_0})t] \{ \Re[\rho_{+-}(0)] \cos(\omega_0 t) - \Im[\rho_{+-}(0)] \sin(\omega_0 t) \}, \\ \Im[\rho_{+-}(t)] &= \exp[-\frac{\Delta^2}{2\omega_0^2}(\gamma_{\omega_0} + \gamma_{-\omega_0})t] \{ \Re[\rho_{+-}(0)] \sin(\omega_0 t) + \Im[\rho_{+-}(0)] \cos(\omega_0 t) \}.\end{aligned}$$

From equations (2.55) and (2.56) one can extract the rate constant for the relaxation of population $\frac{1}{\tau_R} = \frac{\Delta^2}{4\omega_0^2}(\gamma_{\omega_0} + \gamma_{-\omega_0})$ and the dephasing rate $\frac{1}{\tau_D} = \frac{1}{2}\tau_R$ [39]. Here, τ_R and τ_D are the relaxation time and dephasing time of the system respectively.

2.4 Validity of the Secular Approximation

The reasoning of the secular approximation performed in the Markovian master equation (1.35) was the following: If the typical time scale of the system τ_S is much smaller than the relaxation time τ_R , the non-secular terms in the master equation (1.33) oscillate very rapidly during τ_R and can thus be neglected. In the previous chapter the system relaxation time for the spin-boson system was determined from the Markovian time evolution:

$$\tau_R = \frac{4\omega_0^2}{\Delta^2(\gamma_{\omega_0} + \gamma_{-\omega_0})}. \quad (2.57)$$

The typical time scale for the spin-boson model is $\tau_s = \frac{1}{\omega_0}$. Now one can announce the condition for the secular approximation to be valid in the Markovian case:

$$\tau_S \ll \tau_R \quad \Leftrightarrow \quad \gamma_{\omega_0} + \gamma_{-\omega_0} \ll \omega_0 \left(1 + \frac{\epsilon^2}{\Delta^2}\right) \quad \Leftrightarrow \quad \alpha \ll 1. \quad (2.58)$$

In the non-Markovian case the coarse-graining performed by the secular approximation may destroy the non-Markovian memory effects found in the short time

scales. To ensure that the secular approximation is valid also in the non-Markovian regime one needs to compare the time scales of the non-Markovian dynamics, i.e. the environment correlation time scale with the typical time scale of the system defining the time scale of the oscillations left out in the secular approximation. The environment correlation time scale can be written as

$$\tau_c = \frac{1}{\omega_c}, \quad (2.59)$$

with ω_c being the cutoff frequency originally introduced to eliminate infinities in frequency integrations. The cutoff frequency then also determines if the dynamics of the system is non-Markovian. Now the secular approximation is valid in the non-

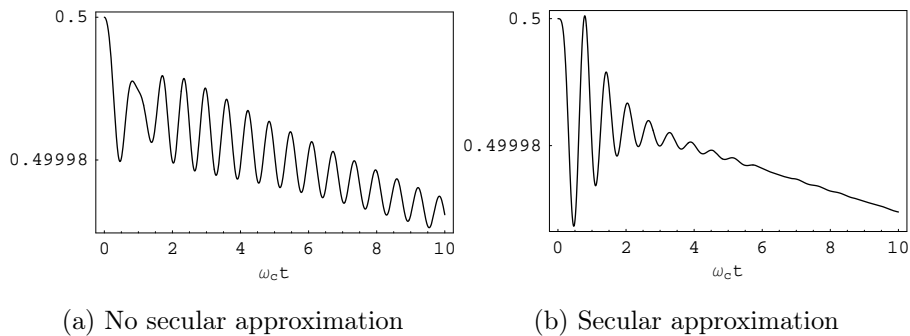


Figure 2.5: Population of state $|\psi_+\rangle$ with parameter values $\alpha = 0.01$, $\frac{\epsilon}{\omega_c} = 1$ and $\frac{\Delta}{\omega_c} = 10$. The initial values of the population and the coherences are $\rho_{++}(0) = 0.5$, $\Re[\rho_{+-}(0) = 0.5]$, $\Im[\rho_{+-}(0)] = 0$.

Markovian regime if the typical time scale of the system τ_s is much smaller than the environment correlation time τ_c :

$$\tau_s \ll \tau_c \quad \Rightarrow \quad \omega_c \ll \omega_0. \quad (2.60)$$

The effect of the coarse-graining can be seen in figures 2.5, 2.6 and 2.7. In the case in figure 2.5 the secular approximation is valid and it does not coarse-grain the

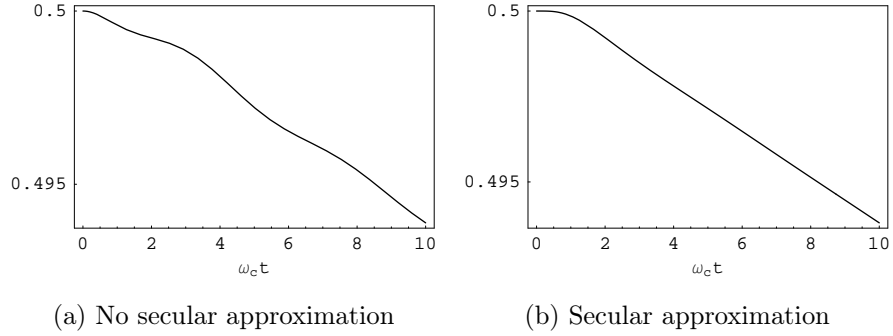


Figure 2.6: Population of state $|\psi_+\rangle$ with $\frac{\epsilon}{\omega_c} = 1$ and $\frac{\Delta}{\omega_c} = 1$. Other parameter values are as in figure 2.5.

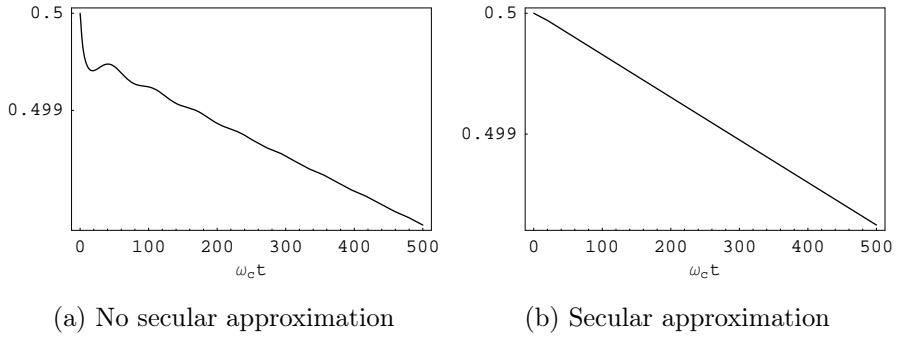


Figure 2.7: Population of state $|\psi_+\rangle$ with $\frac{\epsilon}{\omega_c} = 0.1$ and $\frac{\Delta}{\omega_c} = 0.01$. Other parameter values are as in figure 2.5.

non-Markovian effects. In figure 2.7 the dynamics after the secular approximation is approximately Markovian and the secular approximation does not interfere with the relaxation dynamics.

The validity of the secular approximation was previously studied by comparing the master equation in the case of zero energy bias in section 2.3.2. In the weak coupling case the condition (2.51) can be induced from the time scale condition (2.60).

Chapter 3

Quantum-Jump Approach to Open System Dynamics

Quantum mechanics is usually considered as a theory of ensembles because of its probabilistic nature. The recent possibility to manipulate and observe single particles by using for example ion traps has showed that the ensemble approach is not comprehensive for the description; it is incapable of describing measurements of single particles, where quantum jumps can be observed [40]. Quantum jumps of e.g. trapped ions [41] and light quanta [42] have been demonstrated in experiments.

The quantum jump approach relies on the possibility to apply wave functions rather than density matrices, provided that a stochastic element is included in the evolution of the wave functions. The Monte Carlo wave function method, developed by Klaus Mølmer , Yvan Castin and Jean Dalibard [43, 44, 45] is presented in the following section. The physical interpretation of the stochastic elements in the evolution is discussed and the conditional evolution is related to the measurement theory of quantum mechanics.

In the context of open quantum system the master equation describing the system dynamics may be very complex and impossible to solve by analytical means. The

quantum-jump formalism allows one to simulate the master equation and thus it provides a powerful tool in solving the time evolution of the system. The quantum jump approach may also give new physical insight especially to single-quantum systems.

In the following sections a Monte-Carlo simulation method is developed in order to describe the time-evolution of an open system. The method is introduced for Markovian systems and the equivalence with the master equation approach is proved. A generalization of this method for non-Markovian dynamics is presented and the spin-boson model is studied by means of this approach.

3.1 Monte Carlo Wave-Function Method and Markovian Quantum Jumps

Usually open system dynamics are treated by master equation approach. In the Markovian approximation the master equation describing the dynamics can be written in the form derived in chapter 1.2:

$$\frac{d}{dt}\rho_S = -i[H_S, \rho_S] + \mathcal{D}(\rho_S(t)), \quad (3.1)$$

where the dissipator $\mathcal{D}(\rho_S(t))$ may be written as

$$\mathcal{D}(\tilde{\rho}_S(t)) = \sum_m (C_m \rho_S C_m^\dagger - \frac{1}{2} \{C_m^\dagger C_m, \rho_S\}). \quad (3.2)$$

Here, the constant decay rates are embedded into the operators C_m .

The Monte Carlo wave function method (MCWF) for Markovian systems is based on the evolution of a Monte Carlo wave function of the system consisting of two elements: evolution with a non-Hermitian Hamiltonian and randomly occurring quantum jumps, followed by wave function renormalization.

Assume that the Markovian master equation describing the system dynamics is of the form (3.1). Consider the system at time t in a state with the normalized wave

function $|\phi(t)\rangle$. To determine the wave function at time $t + \delta t$ two steps are carried out:

1. Calculate the wave function $|\phi^{(1)}(t + \delta t)\rangle$ by evolving $|\phi(t)\rangle$ with the non-Hermitian Hamiltonian [43]

$$H = H_S - \frac{i}{2} \sum_m C_m^\dagger C_m. \quad (3.3)$$

The evolved wave function is

$$|\phi^{(1)}(t + \delta t)\rangle = (1 - iH\delta t) |\phi(t)\rangle, \quad \text{for sufficiently small } \delta t. \quad (3.4)$$

The square of the norm of the new wave function is

$$\begin{aligned} \langle \phi^{(1)}(t + \delta t) | \phi^{(1)}(t + \delta t) \rangle &= \langle \phi(t) | (1 + iH^\dagger \delta t)(1 - iH\delta t) | \phi(t) \rangle \\ &= 1 - \delta p, \end{aligned} \quad (3.5)$$

with

$$\delta p = i\delta t \langle \phi(t) | H - H^\dagger | \phi(t) \rangle = \sum_m \delta p_m, \quad (3.6)$$

$$\delta p_m = \delta t \langle \phi(t) | C_m^\dagger C_m | \phi(t) \rangle. \quad (3.7)$$

The size of the step δt has to be adjusted in such way that $\delta p \ll 1$.

2. The second step is the possible quantum jump. Whether the jump occurs or not depends on a quasi-random number r distributed between 0 and 1:

- If $\delta p < r$, no quantum jump occurs and the new normalized wave function is

$$|\phi(t + \delta t)\rangle = \frac{\phi^{(1)}(t + \delta t)}{(1 - \delta p)^{1/2}}. \quad (3.8)$$

- If $\delta p > r$, a quantum jump occurs and the new wave function is

$$|\phi(t + \delta t)\rangle = \frac{C_m |\phi(t)\rangle}{(\delta p_m / \delta t)^{1/2}}, \quad \text{with probability } \delta p_m / \delta p. \quad (3.9)$$

The procedure of propagating a wave function $|\phi(t)\rangle$ in time is equivalent to the master equation (3.1). This can be shown by studying the quantity $\overline{\sigma(t)}$ obtained by averaging $\sigma(t) = |\phi(t)\rangle \langle\phi(t)|$ over all possible outcomes at time t of the MCWF evolutions starting in $|\phi(0)\rangle$. The quantity $\overline{\sigma(t)}$ coincides with the reduced density matrix $\rho_S(t)$.

Consider a MCWF $|\phi(t)\rangle$ at time t . At time $t + \delta t$ the average value of $\sigma(t + \delta t)$ over the evolution caused by different values of the random number r is

$$\begin{aligned} \overline{\sigma(t + \delta t)} &= (1 - \delta p) \frac{|\phi^{(1)}(t + \delta t)\rangle \langle\phi^{(1)}(t + \delta t)|}{1 - \delta p} + \delta p \sum_m \frac{\delta p_m C_m |\phi(t)\rangle \langle\phi(t)| C_m^\dagger}{\delta p} \frac{C_m^\dagger}{\delta p_m / \delta t} \\ &= |\phi^{(1)}(t + \delta t)\rangle \langle\phi^{(1)}(t + \delta t)| + \delta t \sum_m C_m |\phi(t)\rangle \langle\phi(t)| C_m^\dagger. \end{aligned} \quad (3.10)$$

By using equation (3.4) and ignoring terms $\mathcal{O}(\delta t^2)$ the averaged quantity can be written as

$$\overline{\sigma(t + \delta t)} = \sigma(t) - i\delta t [H_S, \sigma(t)] + \delta t \sum_m (C_m \sigma(t) C_m^\dagger - \frac{1}{2} \{C_m^\dagger C_m, \sigma(t)\}). \quad (3.11)$$

By averaging this equation over the possible values of $\sigma(t)$ one obtains

$$\frac{d\bar{\sigma}}{dt} = -i[H_S, \bar{\sigma}] + \mathcal{D}(\bar{\sigma}), \quad (3.12)$$

which is identical to the master equation (3.1).

To give a physical interpretation for the described procedure, it is convenient to study a simple process like the spontaneous emission of a two-level system. Assume the system is at time $t = 0$ in a superposition

$$|\phi(0)\rangle = \alpha_0 |g\rangle + \beta_0 |e\rangle. \quad (3.13)$$

In this simple example the system Hamiltonian is $H_S = \omega_0 \sigma_+ \sigma_-$ and the relaxation operator is $C = \sqrt{\Gamma} \sigma_-$, where Γ is the decay rate describing the rate of the relaxation to the ground state $|g\rangle$. When $t \rightarrow \infty$ the system will be at state $|g\rangle$. This state

could be reached without emitting any photon (probability = $|\alpha_0^2|$) or with the emission of one photon (probability = $|\beta_0^2|$).

In the MCWF formalism the non-Hermitian Hamiltonian (3.3) can be calculated and the evolved wave function is

$$|\phi^{(1)}(\delta t)\rangle = \alpha_0 |g\rangle + \beta_0 e^{-i\omega_0 \delta t} e^{-\Gamma \delta t/2} |e\rangle. \quad (3.14)$$

The probability for a quantum jump to occur can be calculated from equation (3.6)

$$\delta p = \Gamma |\beta_0|^2 \delta t \quad (3.15)$$

and it corresponds to the probability for emitting a photon during δt . The choice of the random number r simulates the result of the measurement of the number of photons emitted between 0 and δt . The occurrence of a random number for which $r < \delta p$ corresponds to a detection of a photon. If a jump occurs the wave function $|\phi(\delta t)\rangle$ is simply $|g\rangle$ and it no longer evolves.

In the case of a random number such that $\delta p < r$ no jump occurs. This corresponds to a measurement with no detection of a photon. Now the normalized wave function is proportional to $|\phi^{(0)}(\delta t)\rangle$ and for small δt it can be written in the form

$$|\phi(\delta t)\rangle = \alpha_0 \left(1 + \frac{\Gamma \delta t}{2} |\beta_0|^2\right) |g\rangle + \beta_0 \left(1 - \frac{\Gamma \delta t}{2} |\alpha_0|^2\right) e^{-i\omega_0 \delta t} |e\rangle. \quad (3.16)$$

From (3.16) one can see that there has been a slight rotation of the wave function: the probability amplitude of being in the ground state $|g\rangle$ has increased, while the probability of being in the excited state $|e\rangle$ has decreased. This change in the probability amplitudes corresponds to the modification of a state when no photon has been detected in a measurement. Thus the information gained in the measurement with no detections has consequences on the evolution of the system. The gained information decreases the probability of an emission of a photon and thus enables the system to evolve without ever emitting one.

3.2 Non-Markovian Quantum Jumps

When studying Markovian dynamics of the system, the memory of the environment is neglected and the past events occurred in the system do not influence the future dynamics. Thus the information the system loses to the environment at the time of a quantum jump is lost forever and the system does not know in what state it was before the jump.

The non-Markovian memory effects make the system dynamics more complex but also give new insight to the physical nature of the problem. A Monte Carlo wave function method, based on the idea of non-Markovian quantum jumps (NMQJ) [15], describes the influence of the memory in an interpretatively clear manner. The concept is based on the idea that the information, which the system loses to the environment at the time of the jump, can be later recovered by the system due to non-Markovian memory. This idea is then formulated as a reversed jump occurring in the dynamics. Other generalizations of the Monte Carlo approach to non-Markovian regime have also been developed. These are based on suitable extensions of the Hilbert space of the system [46, 47, 48]. The non-Markovian quantum jump method is the only stochastic quantum jump process in the reduced system Hilbert space.

As demonstrated in chapter 1 the non-Markovian dynamics of the reduced density matrix ρ_S can be described with the local-in-time master equation

$$\frac{d}{dt}\rho_S(t) = -i[H_S, \rho_S(t)] + \sum_m \gamma_m(t)(C_m \rho(t) C_m^\dagger - \frac{1}{2}\{C_m^\dagger C_m, \rho_S(t)\}), \quad (3.17)$$

where H_S is the system Hamiltonian and C_m are the jump operators describing the changes in the dynamics due to the interaction with the reservoir and $\gamma_m(t)$ is the decay rate of channel m . In the Markovian case the decay rates $\gamma_m(t)$ are positive constants, but in the non-Markovian case the time-dependent functions $\gamma_m(t)$ may get temporarily negative values. This reflects the information flow from

the environment back to the system.

The non-Markovian quantum jump method is very similar to the MCWF method introduced in the previous chapter. The starting point is the local in time master equation (3.17). The central difference between the MCWF and NMQJ methods arises from the temporarily negative decay rates in the non-Markovian case which cause reversed jumps in the single wave function realization. It is convenient to write the master equation in such way that the positive and negative channels are identified at each time t . If the positive channels are indexed with j_+ and the negative channels with j_- and the decay rates are noted with $\gamma_{j_+}(t)$ and $\gamma_{j_-}(t)$ respectively, the master equation reads

$$\begin{aligned} \frac{d}{dt}\rho_S(t) = & -i[H_S, \rho_S(t)] + \sum_{j_+} \gamma_{j_+}(t)(C_{j_+}\rho(t)C_{j_+}^\dagger - \frac{1}{2}\{C_{j_+}^\dagger C_{j_+}, \rho_S(t)\}) \\ & + \sum_{j_-} \gamma_{j_-}(t)(C_{j_-}\rho(t)C_{j_-}^\dagger - \frac{1}{2}\{C_{j_-}^\dagger C_{j_-}, \rho_S(t)\}). \end{aligned} \quad (3.18)$$

Consider an ensemble of wave functions with N members. Assume the N members to share the same initial state $|\phi_0\rangle$. At time t the ensemble density matrix can be written as

$$\rho_S(t) = \sum_{\alpha} \frac{N_{\alpha}}{N} |\phi_{\alpha}(t)\rangle \langle \phi_{\alpha}(t)|, \quad (3.19)$$

where $N_{\alpha}(t)$ is the number of ensemble members in state $|\phi_{\alpha}(t)\rangle$ at time t and N is the total number of state vectors in the ensemble.

In contrast to the MCWF method introduced in the previous chapter there are three steps to consider in order to gain the single state vector $|\phi_{\alpha}(t + \delta t)\rangle$.

1. The deterministic evolution of the state vector, for a sufficiently small time step δt , before the renormalization is given by

$$|\phi_{\alpha}^{(1)}(t + \delta t)\rangle = (1 - iH\delta t) |\phi_{\alpha}(t)\rangle, \quad (3.20)$$

with

$$H = H_S - \frac{i}{2} \sum_{j_+} \gamma_{j_+}(t) C_{j_+}^\dagger C_{j_+} - \frac{i}{2} \sum_{j_-} \gamma_{j_-}(t) C_{j_-}^\dagger C_{j_-}. \quad (3.21)$$

The renormalized wave function is

$$|\phi_\alpha(t + \delta t)\rangle = \frac{|\phi^{(1)}(t + \delta t)\rangle}{\| |\phi^{(1)}(t + \delta t)\rangle \|}. \quad (3.22)$$

2. For positive decay channels the deterministic evolution is interrupted by jumps. If a jump occurs through a positive decay channel j_+ , the renormalized wave function at time $t + \delta t$ is

$$|\phi_\alpha(t + \delta t)\rangle = \frac{C_{j_+} |\phi_\alpha(t)\rangle}{\| C_{j_+} |\phi_\alpha(t)\rangle \|}. \quad (3.23)$$

The jump takes place with probability

$$P_\alpha^{j_+}(t) = \gamma_{j_+}(t) \delta t \langle \phi_\alpha(t) | C_{j_+}^\dagger C_{j_+} | \phi_\alpha(t) \rangle. \quad (3.24)$$

3. For negative decay channels so called reversed jumps occur. The reversed jumps take the system back to the superposition states destroyed earlier by the jumps. These reversed jumps thus resemble the memory present in the environment and this memory, by creation of lost superpositions, allows a recoherence process in the system. The jump operator of the negative channel is of the form

$$D_{\alpha \rightarrow \alpha'}^{j_-}(t) = |\phi_{\alpha'}(t)\rangle \langle \phi_\alpha(t)|, \quad (3.25)$$

with

$$|\phi_\alpha(t)\rangle = \frac{C_{j_-} |\phi'_\alpha(t)\rangle}{\| C_{j_-} |\phi'_\alpha(t)\rangle \|}. \quad (3.26)$$

This transition for a given state vector $|\phi_\alpha(t)\rangle$ occurs with probability

$$P_{\alpha \rightarrow \alpha'}^{j_-}(t) = \frac{N_{\alpha'}(t)}{N_\alpha(t)} |\gamma_{j_-}(t)| \delta t \langle \phi_{\alpha'}(t) | C_{j_-}^\dagger C_{j_-} | \phi_\alpha(t) \rangle. \quad (3.27)$$

For each time step δt a random number r is taken and the evolution of the system depends on the random number as follows:

- If $\sum_{j_+} P_\alpha^{j_+}(t) + \sum_{j_-, \alpha'} P_{\alpha \rightarrow \alpha'}^{j_-}(t) < r$ no jumps occurs and the wave function evolves deterministically.
- If $\sum_{j_+} P_\alpha^{j_+}(t) + \sum_{j_-, \alpha'} P_{\alpha \rightarrow \alpha'}^{j_-}(t) > r$ a jump occurs. The jump probabilities of each channel determine which one of the possible jumps occurs.

The equivalence of this approach with the time convolutionless master equation (3.17) can be shown in a similar way than in the Markovian case. The average value $\bar{\sigma}(t)$ at time $t + \delta t$ over the evolution caused by different values of the random numbers is

$$\begin{aligned}
\overline{\sigma(t + \delta t)} &= \sum_{\alpha} \frac{N_{\alpha}}{N} \left[(1 - \sum_{j_+} P_{\alpha}^{j_+}(t) - \sum_{j_-, \alpha'} P_{\alpha \rightarrow \alpha'}^{j_-}(t)) \frac{|\phi_{\alpha}^{(1)}(t + \delta t)\rangle \langle \phi_{\alpha}^{(1)}(t + \delta t)|}{\| |\phi_{\alpha}^{(1)}(t + \delta t)\rangle \|^2} \right. \\
&\quad + \sum_{j_+} P_{\alpha}^{j_+} \frac{C_{j_+} |\phi_{\alpha}(t)\rangle \langle \phi_{\alpha}(t)| C_{j_+}^{\dagger}}{\| C_{j_+} |\phi_{\alpha}(t)\rangle \|^2} \\
&\quad \left. + \sum_{j_-, \alpha'} P_{\alpha \rightarrow \alpha'}^{j_-}(t) D_{\alpha \rightarrow \alpha'}^{j_-} |\phi_{\alpha}(t)\rangle \langle \phi_{\alpha}(t)| D_{\alpha \rightarrow \alpha'}^{j_- \dagger} \right]. \tag{3.28}
\end{aligned}$$

Using equations (3.20)-(3.27) in (3.28) gives the master equation (3.17) [15].

3.3 Non-Markovian Quantum Jumps and the Spin-Boson Model

The spin-boson model involves three Lindblad operators $C_1 = \sigma_-$, $C_2 = \sigma_+$ and $C_3 = \sigma_z$. The operators C_1 and C_2 generate jumps that affect the populations of the system eigenstates and the operator C_3 produces phase flips. The corresponding decay rates are $\gamma_1(t) = \frac{\Delta^2}{4\omega_0^2} \gamma_{\omega_0}(t)$, $\gamma_2(t) = \frac{\Delta^2}{4\omega_0^2} \gamma_{-\omega_0}(t)$ and $\gamma_3(t) = \frac{\epsilon^2}{4\omega_0^2} \gamma_0(t)$ (c.f. equations (2.26)-(2.30)). The first two decay rates have temporarily negative values while the third decay rate is always positive.

Let us assume that the system is initially in a pure state $|\psi_0(0)\rangle$. Thus all the N ensemble members are initially in the same state. If we ignore the phase flips,

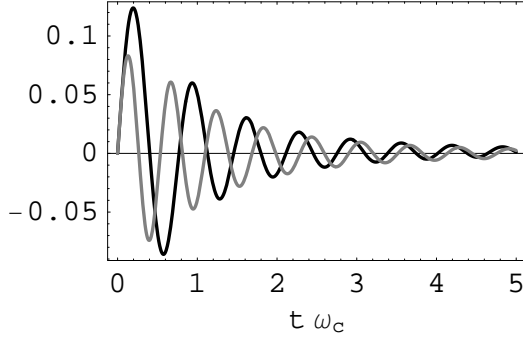


Figure 3.1: Decay rates γ_{ω_0} (black line) and $\gamma_{-\omega_0}$ (gray line) with parameter values $\frac{\omega_0}{\omega_c} = 10$.

i.e., put $\epsilon = 0$, the system has three possible states $|\psi_0(t)\rangle$, $|\psi_+\rangle$ and $|\psi_-\rangle$. Three discrete variables $N_0(t)$, $N_+(t)$ and $N_-(t)$ count the ensemble members on each of these states. Thus initially $N_0(0) = N$ and $N_+(0) = N_-(0) = 0$.

One can see from figure 3.1, that at first both decay rates are positive and thus the Markovian quantum jump description is sufficient. Now the deterministic evolution of the wave function $|\psi_\alpha(t)\rangle$ for a time step δt is generated by the Hamiltonian

$$\begin{aligned} H &= H_S - \frac{i}{2} \sum_{j=1}^3 \gamma_j(t) C_j^\dagger C_j \\ &= \frac{\omega_0}{2} \sigma_z - \frac{1}{2} (\gamma_1(t) |\psi_+\rangle \langle \psi_+| + \gamma_2(t) |\psi_-\rangle \langle \psi_-|). \end{aligned} \quad (3.29)$$

The deterministic evolution is interrupted by jumps. The possible jumps, when both γ_{ω_0} and $\gamma_{-\omega_0}$ are positive are

$$\begin{aligned} |\psi_0(t)\rangle &\longrightarrow |\psi_-\rangle, \quad \text{with probability } p_-^0(t) = \frac{\Delta^2}{4\omega_0^2} \gamma_{\omega_0}(t) \delta t |\langle \psi_0(t) | \psi_+\rangle|^2, \\ |\psi_0(t)\rangle &\longrightarrow |\psi_+\rangle, \quad \text{with probability } p_+^0(t) = \frac{\Delta^2}{4\omega_0^2} \gamma_{-\omega_0}(t) \delta t |\langle \psi_0(t) | \psi_-\rangle|^2, \\ |\psi_+\rangle &\longrightarrow |\psi_-\rangle, \quad \text{with probability } p_-^+(t) = \frac{\Delta^2}{4\omega_0^2} \gamma_{\omega_0}(t) \delta t, \\ |\psi_-\rangle &\longrightarrow |\psi_+\rangle, \quad \text{with probability } p_+^-(t) = \frac{\Delta^2}{4\omega_0^2} \gamma_{-\omega_0}(t) \delta t. \end{aligned} \quad (3.30)$$

The possible jumps are presented in figure 3.2a.

After a certain time the decay rate $\gamma_{-\omega_0}(t)$ becomes negative while the other decay rate $\gamma_{\omega_0}(t)$ remains positive. Now through the positive channel 1 there are still

jumps $|\psi_0(t)\rangle \longrightarrow |\psi_-\rangle$ and $|\psi_+\rangle \longrightarrow |\psi_-\rangle$, but channel 2 now repumps ensemble

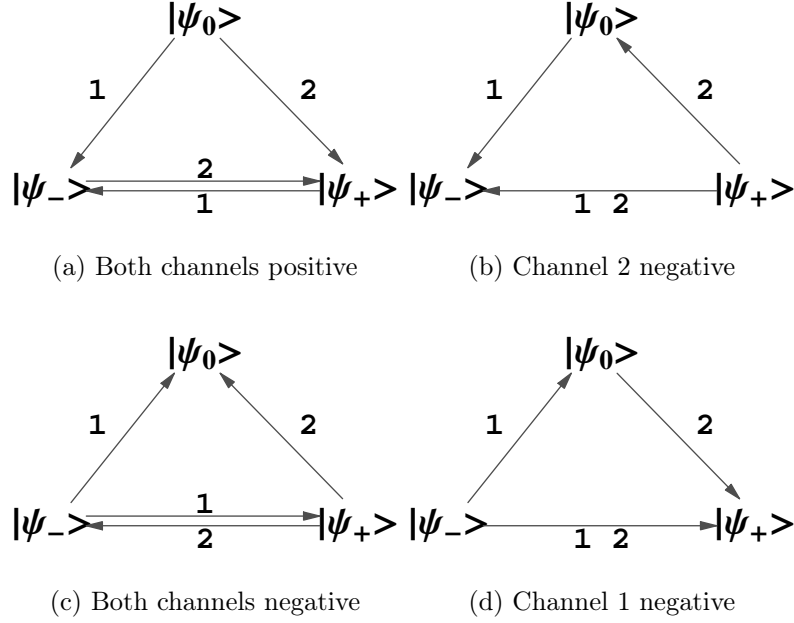


Figure 3.2: Diagrams representing jumps at different times for $\epsilon = 0$

members to $|\psi_0\rangle$ by non-Markovian quantum jumps $|\psi_0\rangle \longleftarrow |\psi_+\rangle$. During this period no ensemble members arrive to $|\psi_+\rangle$ as can be seen in figure 3.2b.

At some point both decay rates become negative and ensemble members are pumped back to $|\psi_0\rangle$ through channels 1 and 2. A diagram describing the jump processes in the case of two negative channels is presented in figure 3.2c. After some time channel 2 becomes positive again. During the time when channel 2 is positive and channel 1 is negative no ensemble members move into $|\psi_-\rangle$. The corresponding dynamics of the probability of the state $|\psi_+\rangle$ in the non-Markovian regime, which is attained from the density matrix formalism, is presented in figure 3.3a. The dynamics of the real part of the off-diagonal element of the density matrix is illustrated in figure 3.3b. One can see that the reproduction of superpositions through jumps $|\psi_0\rangle \longleftarrow |\psi_+\rangle$ and $|\psi_0\rangle \longleftarrow |\psi_-\rangle$ induces recoherence as $\Re[\rho_{+-}]$

temporarily increases.

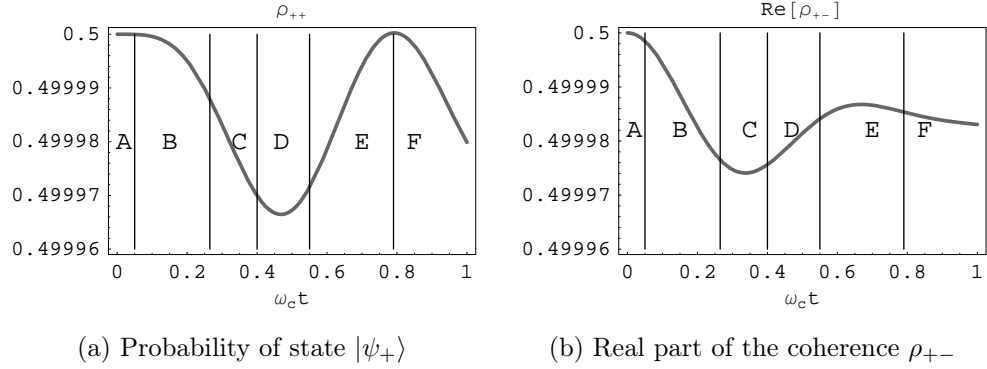


Figure 3.3: The dynamics of (a) the probability of the state $|\psi_+\rangle$ and (b) the real part of the non-diagonal matrix element ρ_{+-} in the non-Markovian regime attained from the density matrix formalism in the interaction picture with the parameter values $\alpha = 0.01$, $\frac{\Delta}{\omega_c} = 10$, $\epsilon = 0$. The initial state is $|\psi_0(0)\rangle = \frac{1}{\sqrt{2}}(|\psi_+\rangle + |\psi_-\rangle)$. The sign of the decay rates in different regions is listed in tabular 3.1.

Region	Decay rates
A	$\gamma_{\omega_0}(t), \gamma_{-\omega_0}(t) > 0, \gamma_{\omega_0}(t) = \gamma_{-\omega_0}(t)$
B	$\gamma_{\omega_0}(t), \gamma_{-\omega_0}(t) > 0, \gamma_{\omega_0}(t) > \gamma_{-\omega_0}(t)$
C	$\gamma_{\omega_0}(t) > 0, \gamma_{-\omega_0}(t) < 0$
D	$\gamma_{\omega_0}(t), \gamma_{-\omega_0}(t) < 0$
E	$\gamma_{\omega_0}(t) < 0, \gamma_{-\omega_0}(t) > 0$
F	$\gamma_{\omega_0}(t) > 0, \gamma_{-\omega_0}(t) < 0$

Table 3.1: Sign of the decay rates.

At some point the non-Markovian memory effects disappear and the decay rates settle into their Markovian value. At zero temperature the Markovian value of the decay rate of channel 2 is zero, i.e. $\gamma_{-\omega_0} = 0$. For channel 1 the corresponding value

is nonzero, i.e. $\gamma_{\omega_0} \neq 0$. Thus, when the decay rates settle into their Markovian values there are neither reversed jumps nor jumps through channel 2. Therefore the only jumps occurring after the non-Markovian regime are $|\psi_+\rangle \longrightarrow |\psi_-\rangle$ and $|\psi_0\rangle \longrightarrow |\psi_-\rangle$. Now all ensemble members go to state $|\psi_-\rangle$ as $t \rightarrow \infty$ and the off-diagonal elements of the density matrix tend to zero because no superpositions are recreated.

To understand the effect of the phase flips occurring in the system dynamics let us study the case with $\epsilon \neq 0$ and $\Delta = 0$, where phase flips are the only possible jumps. In the interaction picture the deterministic evolution does not change the wave function and the only possible jumps are represented by the operator $C_3 = \sigma_z$. The decay rate $\gamma_0(t)$, which determines the jump probability, is always positive and thus only Markovian quantum jumps occur.

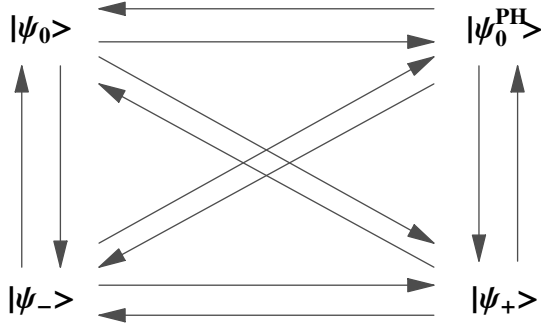


Figure 3.4: All possible states and jumps for a single realization. Here, $|\psi_0\rangle = \alpha_0 |\psi_+\rangle + \beta_0 |\psi_-\rangle$ and $|\psi_0^{\text{PH}}\rangle = \alpha_0 |\psi_+\rangle - \beta_0 |\psi_-\rangle$.

Assume that the system is initially in a pure state $|\psi_0(0)\rangle = \frac{1}{\sqrt{2}}(|\psi_+\rangle + |\psi_-\rangle)$, i.e., all ensemble members have the same relative phase and the off-diagonal density matrix element is $\rho_{+-}(0) = \frac{1}{2}$. Because the deterministic evolution does not affect the dynamics wave function has two possible states: $|\phi_{\text{even}}(t)\rangle = \frac{1}{\sqrt{2}}(|\psi_+\rangle + |\psi_-\rangle)$ and $|\phi_{\text{odd}}(t)\rangle = \frac{1}{\sqrt{2}}(|\psi_+\rangle - |\psi_-\rangle)$, where $|\phi_{\text{even}}(t)\rangle$ is the state if an even number of

phase flips have occurred and $|\phi_{\text{odd}}(t)\rangle$ if there has been an odd number of phase flips. Now the off-diagonal density matrix element can be written as

$$\rho_{+-}(t) = \frac{1}{2} \frac{N_{\text{even}}(t) - N_{\text{odd}}(t)}{N}, \quad (3.31)$$

where N_{even} ($N_{\text{odd}}(t)$) is the number of wave function realizations in state $|\phi_{\text{even}}(t)\rangle$ ($|\phi_{\text{odd}}(t)\rangle$). Because the probability of the occurrence of a phase flip, $p_{\text{PH}} = \gamma_3(t)\delta t$, does not depend on the state that the system is in, the system will eventually be balanced in such way that $N_{\text{even}} = N_{\text{odd}}$ for large N . Thus $\rho_{+-} \rightarrow 0$ as $t \rightarrow \infty$.

When both $\epsilon \neq 0$ and $\Delta \neq 0$, there exists a phase flip counter part for the state $|\psi_0\rangle$. The possible states and jumps are demonstrated in figure 3.4. In figure 3.5 the population of state $|\psi_+\rangle$ and the coherence is plotted for a fixed ratio $\frac{\omega_0}{\omega_c}$ and varying values of $\frac{\epsilon}{\Delta}$. One can see that the population does not change as $\frac{\epsilon}{\Delta}$ varies, but the behavior of the coherence changes.

Let us study the real part of the coherence $\Re[\rho_{+-}] = \frac{1}{N} \sum_{i=1}^N \alpha_i \beta_i^*$, where $|\psi_0^i\rangle = \alpha_i |\psi_+\rangle + \beta_i |\psi_-\rangle$. Jumps $|\psi_0\rangle \rightarrow |\psi_+\rangle$, $|\psi_0\rangle \rightarrow |\psi_-\rangle$, $|\psi_0^{\text{PH}}\rangle \rightarrow |\psi_+\rangle$, $|\psi_0^{\text{PH}}\rangle \rightarrow |\psi_-\rangle$ and phase flips reduce the number of terms in the sum and therefore induce decoherence. Reversed jumps $|\psi_0\rangle \leftarrow |\psi_+\rangle$, $|\psi_0\rangle \leftarrow |\psi_-\rangle$ and $|\psi_0^{\text{PH}}\rangle \leftarrow |\psi_+\rangle$, $|\psi_0^{\text{PH}}\rangle \leftarrow |\psi_-\rangle$ produce new terms into the sum, but if there is an equal amount of reversed jumps to $|\psi_0\rangle$ and $|\psi_0^{\text{PH}}\rangle$ the new terms in the sum cancel each other and no recoherence takes place.

To find out for which values $\frac{\epsilon}{\Delta}$ there is recoherence let us study the quantity $N_0(t) - N_0^{\text{PH}}(t)$. Here, $N_0(t)$ is the number of ensemble members in state $|\psi_0\rangle$ and $N_0^{\text{PH}}(t)$ the number of elements in state $|\psi_0^{\text{PH}}\rangle$. The real part of the coherence is an increasing function, when $N_0(t) - N_0^{\text{PH}}(t)$ is increasing, and a decreasing function when $N_0(t) - N_0^{\text{PH}}(t)$ is decreasing. Let the initial state be $|\psi_0(0)\rangle = \alpha_0 |\psi_+\rangle + \beta_0 |\psi_-\rangle$. Let us study the cases with different positive and negative channels:

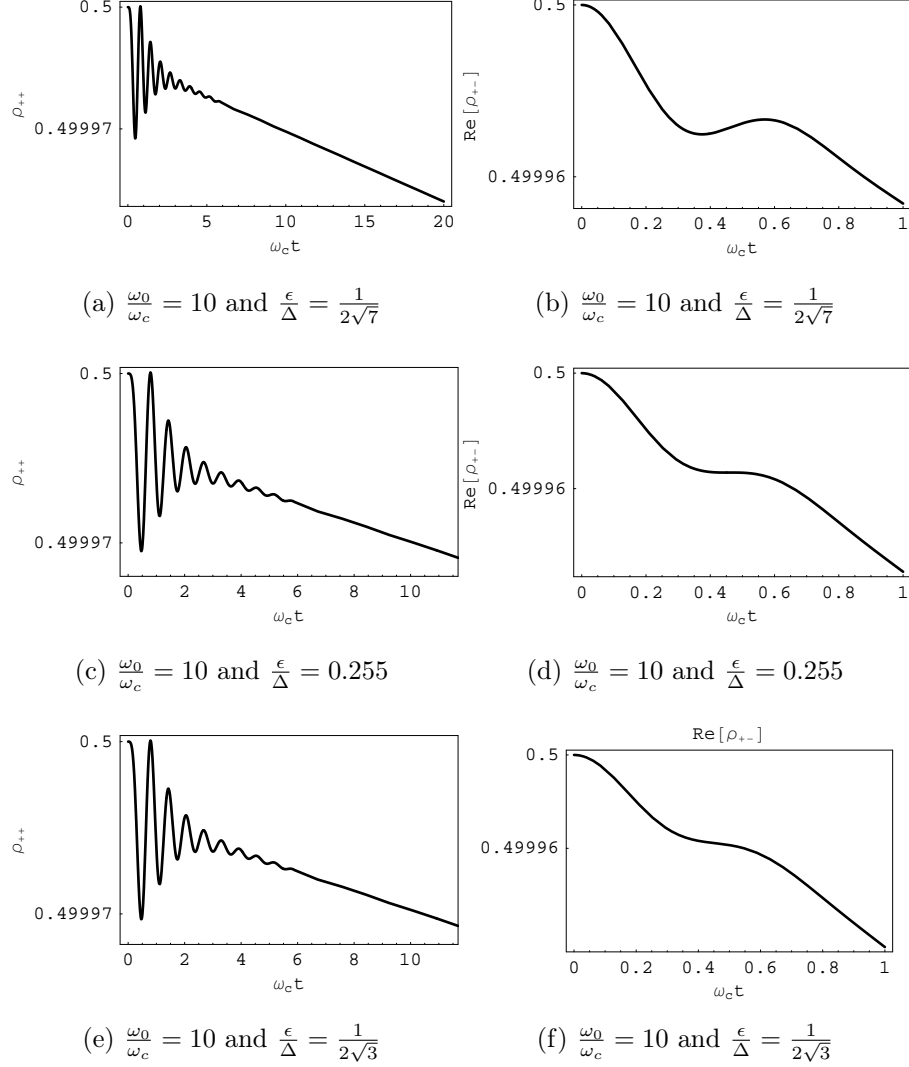


Figure 3.5: The population ρ_{++} of state $|\psi_+\rangle$ [(a), (c) and (e)] and coherence $\Re[\rho_{+-}]$ [(b), (d) and (f)] for different parameter values in the case of a structured reservoir, i.e. $\frac{\omega_0}{\omega_c} = 10$. Here, the coupling constant is $\alpha = 0.01$ and the initial state is $|\psi_0(0)\rangle = \frac{1}{\sqrt{2}}(|\psi_+\rangle + |\psi_-\rangle)$.

$$\gamma_{\omega_0}, \gamma_{-\omega_0} > 0:$$

$$N_0(t + \delta t) - N_0^{\text{PH}}(t + \delta t) < N_0(t) - N_0^{\text{PH}}(t) \quad (3.32)$$

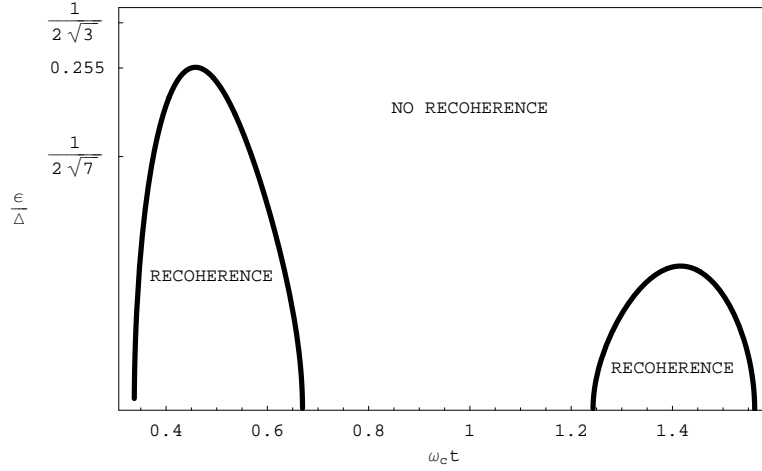


Figure 3.6: The time regions for recoherence for different values of $\frac{\epsilon}{\Delta}$. Here, $\frac{\omega_0}{\omega_c} = 10$, $\alpha = 0.01$ and $\alpha_0 = \beta_0 = \frac{1}{\sqrt{2}}$. The values of $\frac{\epsilon}{\Delta}$ used in figure 3.5 are marked in the plot.

\Rightarrow No recoherence.

$\gamma_{\omega_0} > 0, \gamma_{-\omega_0} < 0$:

$$N_0(t + \delta t) - N_0^{\text{PH}}(t + \delta t) = \underbrace{\left[\frac{\Delta^2}{4\omega_0^2} (|\gamma_{-\omega_0}(t)|\alpha_0^2 - \gamma_{\omega_0}(t)\beta_0^2)\delta t - 2p_{\text{PH}}(t) \right]}_{f(t)} \times (N_0(t) - N_0^{\text{PH}}(t)) \quad (3.33)$$

\Rightarrow Recoherence, if $f(t) > 0$.

$\gamma_{\omega_0}, \gamma_{-\omega_0} < 0$:

$$N_0(t + \delta t) - N_0^{\text{PH}}(t + \delta t) = \underbrace{\left[\frac{\Delta^2}{4\omega_0^2} (|\gamma_{-\omega_0}(t)|\alpha_0^2 + |\gamma_{\omega_0}(t)|\beta_0^2)\delta t - 2p_{\text{PH}}(t) \right]}_{g(t)} \times (N_0(t) - N_0^{\text{PH}}(t)) \quad (3.34)$$

\Rightarrow Recoherence, if $g(t) > 0$.

$\gamma_{\omega_0} < 0, \gamma_{-\omega_0} > 0$:

$$\begin{aligned}
N_0(t + \delta t) - N_0^{\text{PH}}(t + \delta t) &= \underbrace{\left[\frac{\Delta^2}{4\omega_0^2} (|\gamma_{\omega_0}(t)|\beta_0^2 - \gamma_{-\omega_0}(t)\alpha_0^2)\delta t - 2p_{\text{PH}}(t) \right]}_{h(t)} \\
&\times (N_0(t) - N_0^{\text{PH}}(t)) \tag{3.35}
\end{aligned}$$

\Rightarrow Recoherence, if $h(t) > 0$.

Figure 3.6 illustrates for which values of $\frac{\epsilon}{\Delta}$ recoherence occurs for a fixed value $\frac{\omega_0}{\omega_c}$. One can see that as the energy bias ϵ becomes larger compared with the tunneling amplitude Δ the probability of a phase flip increases. As more phase flips occur a reversed jump to $|\psi_0^{\text{PH}}\rangle$ gets as probable as a reversed jump to state $|\psi_0\rangle$, which then causes the system to decohere.

Chapter 4

Applications for the spin-boson model

4.1 Double-well system

The double-well system is a more general system than the two-level system and it has therefore more applications than the simple spin-system. It can be truncated into a two-state system under certain conditions and thereby studied with the spin-boson model. The double-well system and the truncation procedure has been extensively studied in the review [3].

The double-well system is described by a continuous degree of freedom q , e.g. a geometrical coordinate, and a potential energy function $V(q)$ with two separate minima. A schematic picture of the system is presented in figure 4.1. The barrier

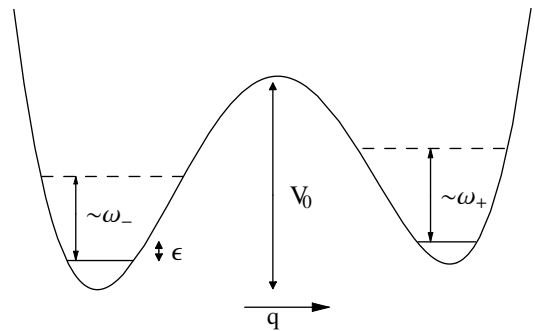


Figure 4.1: The double-well system.

height is such that $V_0 \gg \omega_A$, where ω_A is of the order of the classical small-oscillation frequencies ω_+ and ω_- . In this case, the quantum motion in either well separately is semiclassical and the separation of the first excited state of the well from the ground state is approximately ω_+ (or ω_-) of order ω_A . If the detuning ϵ between the ground states is small compared to ω_A , then for small temperatures $T \ll \omega_A$ the system can be restricted to a two-dimensional Hilbert space spanned by the two ground states.

There is also the possibility of tunneling between the two wells. The matrix element for this process is Δ_0 . For the tunneling not to mix the ground states of the two dimensional Hilbert space with the excited states of the system, the tunneling matrix element has to be such that $\Delta_0 \ll \omega_A$. Now the Hamiltonian of the system can be written as a Hamiltonian for the two-state system, i.e.

$$H = -\frac{1}{2}\Delta_0\sigma_x + \frac{1}{2}\epsilon\sigma_z, \quad (4.1)$$

with the basis chosen such that the eigenstate of σ_z with eigenvalue $+1$ corresponds to the system being localized in the right well.

In most cases of experimental interest the coupling of the system to its environment is through a term of the form $\sigma_z \otimes E$, where E is an operator of the environment. A coupling of this form means that the state of the environment is sensitive to the value of σ_z . In the case of such coupling the Hamiltonian of the compound system is the spin-boson Hamiltonian

$$H_{SB} = -\frac{1}{2}\Delta\sigma_x + \frac{1}{2}\epsilon\sigma_z + \sum_{\alpha} \left(\frac{1}{2}m_{\alpha}\omega_{\alpha}x_{\alpha}^2 + \frac{p_{\alpha}^2}{2m_{\alpha}} \right) + \frac{1}{2}q_0\sigma_z \sum_{\alpha} c_{\alpha}x_{\alpha}, \quad (4.2)$$

where Δ is a ‘‘bare’’ tunneling matrix element, ϵ is the energy bias, m_{α} , ω_{α} , x_{α} , p_{α} are, respectively, the mass, frequency, coordinate and momentum of the α th harmonic oscillator of the environment, and q_0 is a parameter which represents the the distance between the two potential minima. For a system, which is primarily

a two-state one, the parameter q_0 is superfluous. c_α represents the strength of the coupling of the system to the α th oscillator.

Complete information about the effect of the environment is included in the spectral function

$$J(\omega) \equiv \frac{\pi}{2} \sum_{\alpha} \frac{c_{\alpha}}{m_{\alpha}\omega_{\alpha}} \delta(\omega - \omega_{\alpha}). \quad (4.3)$$

For a truncated two-state system the form of $J(\omega)$ is obtained from a knowledge of the classical equation of motion of the system, and the choice of the “bare” tunneling matrix element is not independent of the system. $J(\omega)$ is a smooth function of ω and it is of the form ω^s up to some frequency ω_c . For the truncated two-state system the quantity ω_c enters in a natural way as a cutoff due to the truncation procedure. For the truncation to be valid the conditions

$$\frac{\epsilon}{\omega_c} \ll 1, \quad \frac{\Delta}{\omega_c} \ll 1, \quad \frac{kT}{\omega_c} \ll 1 \quad (4.4)$$

need to be fulfilled [3].

4.2 Double quantum dot charge qubit

Quantum dots are semiconductor structures containing a small number of electrons ($1 \sim 1000$) within a region of space of the size on the scale of sub-micrometers [4]. Many properties of such systems can be investigated by transport, e.g. current-voltage measurements, if the dots are fabricated between contacts acting as source and drain for electrons entering or leaving the dot. By changing the size or the shape of the dot one can consider dots as artificial atoms representing different atoms of the periodic table. Quantum effects present in atoms, such as discrete energy levels and quantum chaos, are observable in quantum dots in a controllable manner [49]. These properties make quantum dots very useful for measurements.

There are three effects dominating transport through quantum dots: the tunnel effect, where electrons penetrate an electronic potential, the charging effect due to

the discreteness of the electronic charge, and size quantization originating from the smallness of the dots. The charging effect, also called Coulomb blockade effect, is the most important out of these three and it explains the simplest experiments on quantum dots.

Coupling of two quantum dots leads to double quantum dots, sometimes referred to as artificial molecules, although this terminology might be misleading. In the strong Coulomb blockade limit double quantum dots are better described as two-level systems with controllable level spacing and one additional transport electron. This type of structure is referred to as the double quantum dot charge qubit.

4.2.1 Double Dot Model

The simplest model defines a double quantum dot as a composite system of two individual dots connected through a static tunnel barrier. The dots are labeled as left (L) and right (R) dot. The effective qubit Hilbert space is assumed to be $\mathcal{H}^{(2)} = \text{span}\{|L\rangle, |R\rangle\}$, with the many-body states $|L\rangle = |N_L + 1, N_R\rangle$ and $|R\rangle = |N_L, N_R + 1\rangle$ with energies ϵ_L and ϵ_R , corresponding to the lowest energy states for one additional electron in the left or the right dot. The empty ground state $|0\rangle = |N_L, N_R\rangle$ has one electron less. The left-right degree of freedom in $\mathcal{H}^{(2)}$ defines a pseudo-spin 1/2 and thus the inter-dot tunneling between the left and the right dot can be described by the Hamiltonian

$$H_{\text{dot}} = \epsilon_L n_L + \epsilon_R n_R + T_c(p + p^\dagger). \quad (4.5)$$

Here, $n_i = |i\rangle\langle i|$, $i = L, R$, $p = |L\rangle\langle R|$ and T_c is a real parameter describing the tunneling process. By choosing the zero of energy to be $\frac{\epsilon_L + \epsilon_R}{2}$ the Hamiltonian of the qubit can be written as the Hamiltonian of a two-state system

$$H_{\text{TLS}} = \frac{\epsilon}{2}\sigma_z + T_c\sigma_x, \quad (4.6)$$

with $\epsilon = \epsilon_L - \epsilon_R$, $\sigma_z = n_L - n_R$ and $\sigma_x = p + p^\dagger$. The eigenstates of this Hamiltonian are

$$|\pm\rangle = \frac{1}{N_\pm}(\pm 2T_c |L\rangle + (\omega_0 \mp \epsilon) |R\rangle), \quad (4.7)$$

with $\omega_0 = \sqrt{\epsilon^2 + 4T_c^2}$ and $N_\pm = \sqrt{4T_c^2 + (\omega_0 \mp \epsilon)^2}$. These eigenstates correspond to hybridized wave functions, i.e. bonding and antibonding states of the localized states $|L\rangle$ and $|R\rangle$.

In the regime of strong Coulomb blockade the double quantum dot can be tuned into a regime that is governed by the spin-boson model [50, 51, 52]:

$$H = \frac{\epsilon}{2}\sigma_z + T_c\sigma_x + \frac{1}{2}\sigma_z \sum_Q g_Q(a_Q + a_Q^\dagger) + \sum_Q \omega_Q a_Q^\dagger a_Q. \quad (4.8)$$

Here, a_Q :s are the annihilation operators of the bosonic environment that the double quantum dot is interacting with. The boson spectral density determining the type of the interaction of the double dot with the environment is the key quantity in the description of the double quantum dot dynamics.

4.2.2 Boson Spectral Density

Boson spectral density $J(\omega) = \sum_Q |g_Q|^2 \delta(\omega - \omega_Q)$ is the only quantity describing the interaction between the system and its environment. It fully determines the correlation function and the decay rates in the final master equation describing the dynamics of the double quantum dot. There are two kinds of models of spectral function $J(\omega)$:

(A) Phenomenological parametrization:

This is the Spin-Boson Model -parametrization

$$J(\omega) = \frac{\alpha}{2} \omega_{\text{ph}}^{1-s} \omega^s e^{-\omega/\omega_c}, \quad (4.9)$$

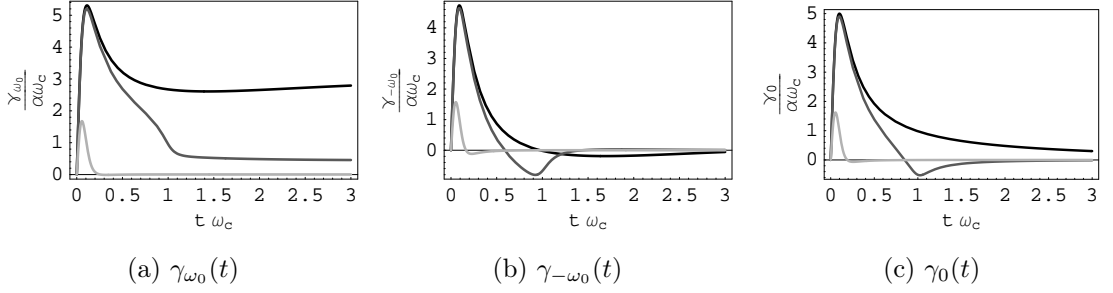


Figure 4.2: Decay rates for the piezoelectric spectral density with $\frac{\omega_0}{\omega_c} = 0.1$. The decay rates are presented for three different parameter values in each plot: $\omega_d/\omega_0 = 0.1$ (black line), $\omega_d/\omega_0 = 1$ (dark gray line), $\omega_d/\omega_0 = 10$ (light gray line).

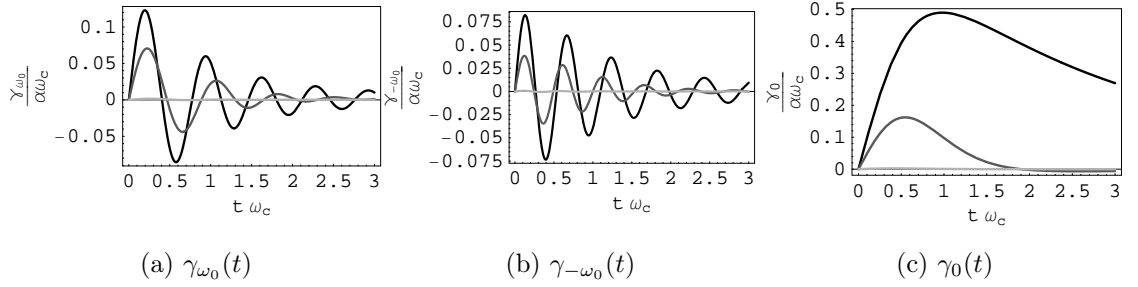


Figure 4.3: Decay rates for the piezoelectric spectral density with $\frac{\omega_0}{\omega_c} = 10$. The decay rates are presented for three different parameter values in each plot: $\omega_d/\omega_0 = 0.1$ (black line), $\omega_d/\omega_0 = 1$ (dark gray line), $\omega_d/\omega_0 = 10$ (light gray line).

where ω_{ph} is a reference frequency introduced to make the coupling constant α dimensionless. Here, the case $0 \leq s < 1$ corresponds to sub-Ohmic, $s = 1$ to Ohmic and $s > 1$ to super-Ohmic case.

(B) Microscopic models for specific forms of electron-boson interaction: Microscopic models are more restricted towards some specific situations but can yield interesting insight into the dissipation mechanism in the respective system. For example the coupling of bulk acoustic phonons to a electron charge

density has been widely studied [50, 51, 52, 53, 54, 55]. For a piezoelectric coupling the spectral density reads [4]

$$J^{\text{pz}}(\omega) = g_{\text{pz}}\omega\left(1 - \frac{\omega_d}{\omega} \sin\left(\frac{\omega}{\omega_d}\right)\right)e^{-\omega/\omega_c}. \quad (4.10)$$

Here, g_{pz} is a coupling constant and $\omega_d = \frac{c_s}{d}$, where c_s is the speed of sound and d is the distance between the dots. There is one additional time scale in the system, defined by ω_d , compared with the Ohmic case. The decay rates resulting from this type of spectral density are plotted in figures 4.2 and 4.3. When the time scales are such that $\omega_d \ll \omega_0$ the dynamics is equivalent with the Ohmic case.

4.3 Biomolecular systems and the Spin-Boson Model

Quantum mechanics plays an important role in many biological systems [56]. Because the systems of interest are without exception open, it is necessary to know how the environment influences the functionality of the biological system. This can be described by quantum mechanical open system models. Biological systems are also useful from experimental point of view, because biomolecules are efficient, controllable and refined quantum mechanical nanoscale devices whose complexity cannot be fabricated even with the most advanced nanotechnology [57].

The spin-boson model can be applied to systems of coupled biomolecules. The model is naturally a simplified model of the actual biomolecules and their environment, but it describes all the essential features of the system.

4.3.1 Model for Individual Chromophores with the Solvent

A chromophore is an optically active biomolecule. A natural environment for the chromophore consists of solvent and protein. The coupling of the electronic exci-

tations in the chromophore to its environment may be modeled by an independent boson model with the total system Hamiltonian [56]

$$H = \frac{\epsilon_1}{2}\sigma_z^1 + \sum_{\alpha} \omega_{\alpha} a_{\alpha}^{\dagger} a_{\alpha} + \sigma_z^1 \sum_{\alpha} c_{\alpha} (a_{\alpha} + a_{\alpha}^{\dagger}). \quad (4.11)$$

Thus the chromophore is modeled as a two-level system with energy gap ϵ_1 between its ground and excited state and the environment consisting of the surrounding solvent and protein is modeled as a bath of harmonic oscillators. The coupling to the environment is determined by the spectral density $J(\omega)$. The spectral density can be obtained from the microscopic details of the model under consideration.

The simplest model arises when the chromophore is treated as a point dipole inside a uniform, spherical protein surrounded by a uniform polar (i.e. dielectric constant < 15) solvent. If the protein has a static dielectric constant, the spectral density is of the form [56]

$$J(\omega) = \frac{(\Delta\mu)^2}{4\pi\epsilon_0 b^3} \Im \frac{2(\epsilon(\omega) - \epsilon_p)}{2\epsilon(\omega) + \epsilon_p}, \quad (4.12)$$

where b is the radius of the protein containing the chromophore, $\epsilon(\omega)$ is the dielectric function of the solvent and ϵ_p is a dielectric constant of representing the protein environment. $\Delta\mu$ is the difference between the dipole moment of the chromophore in the ground and excited states. For a Debye solvent the spectral density is of the form [58]

$$J(\omega) = \frac{(\Delta\mu)^2}{4\pi\epsilon_0 b^3} \frac{6\epsilon_p(\epsilon_s - \epsilon_{\infty})}{(2\epsilon_s + \epsilon_p)(2\epsilon_{\infty} + \epsilon_p)} \frac{\omega\tau_E}{\omega^2\tau_E^2 + 1}, \quad (4.13)$$

where ϵ_s and ϵ_{∞} are the static and high frequency dielectric constants of the solvent, respectively, and $\tau_E = \frac{2\epsilon_{\infty} + \epsilon_p}{2\epsilon_s + \epsilon_p} \tau_D$, where τ_D is the Debye relaxation time of the solvent.

4.3.2 Model for Two Biomolecules

Consider now two biomolecules coupled by the Förster interaction Δ [58]. The total Hamiltonian can be written as a sum of two spin-boson Hamiltonians of each

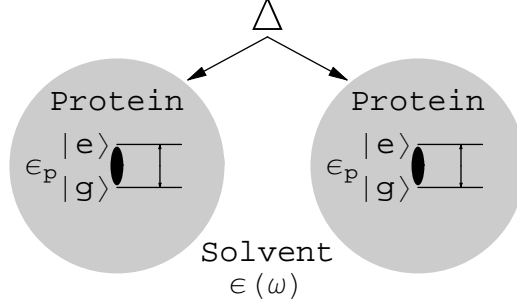


Figure 4.4: Two chromophores (black dots) with energy gaps ϵ_1 and ϵ_2 coupled with an interaction energy Δ due to the Förster dipole-dipole interaction. The chromophores are centered inside spherical proteins with static dielectric constant ϵ_p and surrounded by a polar solvent with dielectric function $\epsilon(\omega)$.

chromophore [56]:

$$H = \frac{\epsilon_1}{2}\sigma_z^1 + \frac{\epsilon_2}{2}\sigma_z^2 + (\Delta\mu_1)\sigma_z^1 R_1 + (\Delta\mu_2)\sigma_z^2 R_2 + \Delta(\sigma_x^1\sigma_x^2 + \sigma_y^1\sigma_y^2) + B_1 + B_2, \quad (4.14)$$

where $R_i = \sum_{\alpha} c_{i,\alpha}(a_{i,\alpha} + a_{i,\alpha}^{\dagger})$ and $B_i = \sum_{\alpha} \omega_{i,\alpha}(a_{i,\alpha}^{\dagger} a_{i,\alpha})$, ($i = 1, 2$).

Mapping to Spin-Boson Model

The method used to map the model of two biomolecules into the spin-boson model is the same as the one used for coupled quantum dots or other qubit systems. The number of excitations in the system is related to the operator $N = \frac{1}{2}(\sigma_z^1 + \sigma_z^2 + 2)$, which commutes with the Hamiltonian. Thus the number of excitations in the system is constant. If we assume that the number of excitations in the system is only one, then $N|\psi\rangle = |\psi\rangle$ and one can project onto the corresponding two-dimensional subspace $\{|e\rangle \otimes |g\rangle, |g\rangle \otimes |e\rangle\}$. Now the composite system Hamiltonian can be written as

$$H = \frac{\epsilon}{2}\sigma_z + \frac{\Delta}{2}\sigma_x + \sigma_z V + \sum_{\alpha,i} \omega_{i,\alpha} a_{i,\alpha}^{\dagger} a_{i,\alpha}, \quad (4.15)$$

with $V = (\Delta\mu_1)R_1 - (\Delta\mu_2)R_2$ and $\epsilon = \epsilon_1 - \epsilon_2$. If the molecules are far apart, the bath modes coupled to each chromophore are independent, i.e. $[a_{1,\alpha}, a_{2,\beta}^\dagger] = 0$, and the environment can be modeled as a set of independent harmonic oscillators. The final Hamiltonian thus reads

$$H = \frac{\epsilon}{2}\sigma_z + \frac{\Delta}{2}\sigma_x + \sigma_z \sum_{\beta} d_{\beta}(a_{\beta}^{\dagger} + a_{\beta}) + \sum_{\beta} \omega_{\beta} a_{\beta}^{\dagger} a_{\beta}. \quad (4.16)$$

To complete the description one needs to determine the spectral density $J(\omega)$ specifying the interaction between the system and the environment. For the case of a Debye dielectric (4.13) the system has an Ohmic spectral density [58], i.e. $J(\omega) = \alpha\omega e^{-\omega/\omega_c}$ with the dimensionless coupling constant

$$\alpha = \frac{1}{2\pi\epsilon_0 h} \left[\frac{(\Delta\mu_1)^2}{b_1^3} + \frac{(\Delta\mu_2)^2}{b_2^3} \right] \frac{6\epsilon_p(\epsilon_s - \epsilon_{\infty})\tau_D}{(2\epsilon_s + \epsilon_p)^2}. \quad (4.17)$$

For a chromophore in water the coupling constant is $\alpha \approx 1$, but the protein shielding the chromophore reduces the coupling constant to $\alpha \approx 0.01$. Thus the weak coupling approximation can be performed in deriving a master equation for the biomolecular systems. The parameter region $\Delta > \omega_c$ is relevant for biomolecular systems and thus a non-Markovian treatment of the dynamics is necessary [58].

Chapter 5

Conclusions

We have derived a time convolutionless non-Markovian master equation describing the open system dynamics of the spin-boson model with the view to studying the microscopic processes inducing the behavior of the two-level system in short time scales using the non-Markovian quantum jump approach. The derivation of the master equation was performed by using the second order time convolutionless projection operator method. The benefit of this approach is that it produces ordinary differential equations describing the system density matrix dynamics in contrast to other approaches resulting in integro-differential equations requiring the use of Laplace transformations in the solution.

The derived master equation is of second order and the secular approximation has been performed. The secular approximation neglects fast rotating terms from the master equation and thus restricts the field of application of the master equation to a particular region of the parameter space. Because we are interested in the non-Markovian behavior of the system the time scales must be such that the secular approximation does not coarse-grain the non-Markovian oscillations occurring in the correlation time scale. This is the case when the system eigenfrequency ω_0 differs by many orders of magnitude from the cutoff frequency ω_c .

We have considered the case with the environment in zero temperature. This assumption yields an analytical expression for the decay rates in the master equation, but one could also determine the decay rates with the temperature dependence by numerical integration and thereby study the effect of temperature on the system. The final master equation derived in this thesis is of the non-Lindblad form with temporarily negative decay rates embodying the memory present in the environment.

The non-Markovian quantum jump method (NMQJ) is presented in section 3. The description is mathematically represented by wave functions instead of density matrices. It gives the wave function a conditional time evolution consisting of a deterministic element and randomly occurring jumps. The method relates the negative decay rates present in the master equation with the recreation of superpositions in the level of single wave functions. By averaging over all the possible realizations of the system one ends up with the density matrix description of the dynamics.

In the case of the spin-boson model there exists three different jump channels for the wave function. Two of these jump processes affect the populations, i.e. the diagonal elements of the system density matrix, and the corresponding decay rates have temporarily negative values. These negative values cause recreation of superpositions in a single wave function realization and can be seen as oscillations in the non-Markovian time scale in the density matrix representation. One of the jumps represents phase flips in the wave function inducing a decoherence process in the density matrix representation. The other two channels with temporarily negative decay rates can cause the non-diagonal elements of the density matrix to increase due to the recreation of superpositions. This process is called recoherence.

The spin-boson model gives an effective description of many real world systems thus providing the possibility of experimental realizations. The last chapter of this thesis is focused on these possible applications of the spin-boson model. The possibility of truncation of a more general double-well system in low temperatures into

the two-level system described by the spin-boson model was studied in the first part of the last chapter. The two other parts of the last section consider different realizations of controllable qubits. The other consisting of mesoscopic semiconductor structures and the other of optically active biomolecules. The spin-boson model describes the essential processes occurring in these systems.

Bibliography

- [1] H.-P. Breuer and F. Petruccione, *The Theory of Open Quantum Systems* (Oxford University Press, Oxford, 2002).
- [2] U. Weiss, *Quantum Dissipative Systems 2nd ed.* (World Scientific, Singapore, 1999).
- [3] A.J. Leggett *et al.*, Rev. Mod. Phys. **59**, 1 (1987).
- [4] T. Brandes, Phys. Rep. **408**, 315 (2005).
- [5] A. Garg, J.N. Onuchic, V.J. Ambegaokar, J. Chem. Phys. **83**, 4491 (1985).
- [6] J. Gilmore, R.H. McKenzie, J. Phys. Chem. A **112**, 2162 (2008).
- [7] T.O. Cheche, S.H. Lin, Phys. Rev. E **64**, 061103 (2001).
- [8] F.K. Wilhelm, S. Kleff, J. von Delft, Chem. Phys. **296**, 345 (2003).
- [9] D.P. DiVincenzo, D. Loss, Phys. Rev. B **71**, 035318 (2005).
- [10] P. Chovsta, J. Phys. A: Math. Gen. **22**, 3927 (1989).
- [11] M. Grifoni, E. Paladino, U. Weiss, Eur. Phys. J. B **10**, 719 (1999).
- [12] M. Grifoni, M. Winterstetter, U. Weiss, Phys. Rev. E **56**, 334 (1997).
- [13] V. Privman, Mod. Phys. Lett. B **16**, 459 (2002).

- [14] V. Privman, J. Stat. Phys. **110**, 957 (2003).
- [15] J. Piilo, S. Maniscalco, K. Härkönen and K.-A. Suominen, Phys. Rev. Lett. **100**, 180402 (2008).
- [16] M. Schlosshauer, Rev. Mod. Phys. **76**, 1267 (2004).
- [17] L.E. Ballentine, *Quantum Mechanics-A Modern Development* (World Scientific, Singapore, 1998).
- [18] E. Prugovečki, *Quantum Mechanics in Hilbert Space* (Academic Press, New York, 1971).
- [19] M. Reed, B. Simon, *Methods of Modern Mathematical Physics II* (Academic Press, New York, 1975).
- [20] R. Alicki, K. Lendi, *Quantum Dynamical Semigroups and Applications* (Springer, Berlin Heidelberg, 2007).
- [21] E.B. Davies, *Quantum Theory of Open Systems* (Academic Press, New York, 1976).
- [22] V. Gorini, A. Kossakowski, E.C.G. Sudarshan, J. Math. Phys. **17**, 821 (1976).
- [23] G. Lindblad, Comm. Math. Phys. **48**, 119 (1976).
- [24] C. Cohen-Tannodji *et al.*, *Atom-Photon Interactions* (Wiley Science Paperback Series, Hoboken NJ, 1998).
- [25] S. Nakajima, Progr. Theor. Phys. **20**, 948 (1958).
- [26] R. Zwanzig, J. Chem. Phys. **33**, 1338 (1960).
- [27] F. Shibata *et al.*, J. Stat. Phys. **17**, 171 (1977).

- [28] J. Piilo *et al.*, arXiv:0902.3609 (2009).
- [29] H.-P. Breuer, J. Piilo, EPL **85**, 50004 (2009).
- [30] A.J. Wonderen, K. Lendi, J. Stat. Phys. **100**, 633 (2000).
- [31] S. Tasaki *et al.*, Ann. Phys. **322**, 631 (2007).
- [32] A. Ishizaki, Y. Tanimura, Chem. Phys **347**, 185 (2008).
- [33] F. Shibata, N. Hashitsume, Z. Phys. B **34**, 197 (1979).
- [34] P. Lambropoulos, D. Petrosyan, *Fundamentals of Quantum Optics and Quantum Information* (Springer, Berlin Heidelberg, 2007).
- [35] W.H. Zurek, Rev. Mod. Phys. **75**, 715 (2003).
- [36] G.M. Palma, K.-A. Suominen, A.K. Ekert, Proc. R. Soc. Lond. A **452**, 567 (1996).
- [37] M. Schlosshauer, *Decoherence and the quantum-to-classical transition* (Springer, Berlin Heidelberg New York, 2007).
- [38] J.P. Paz, W.H. Zurek, Phys. Rev. Lett. **82**, 5181 (1999).
- [39] B.B. Laird, J. Chem. Phys. **94**, 4391 (1991).
- [40] M.B. Plenio, P.L. Knight, Rev. Mod. Phys. **70**, 101 (1998).
- [41] J.C. Bergquist *et al.*, Phys. Rev. Lett. **57**, 1699 (1986).
- [42] S. Gleyzes *et al.*, Nature **446**, 297 (2007).
- [43] K. Mølmer, Y. Castin, J. Dalibard, J. Opt. Soc. Am. B **10**, 524 (1993).
- [44] J. Dalibard, Y. Castin, K. Mølmer, Phys. Rev. Lett. **68**, 580 (1992).

- [45] Y. Castin, J. Dalibard, K. Mølmer, Atomic Physics XIII, 143 (1992).
- [46] A. Imamoglu, Phys. Rev. A **50**, 3650 (1994).
- [47] B. Garraway, Phys. Rev. A **55**, 2290 (1997).
- [48] H.-P. Breuer, Phys. Rev. A **70**, 012106 (2004).
- [49] L. Kouwenhoven, C. Marcus, Phys. World June, 35 (1998).
- [50] T. Brandes, T. Vorrath, Int. J. Mod. Phys. B **17**, 5465 (2003).
- [51] T. Brandes, B. Kramer, Phys. Rev. Lett. **83**, 3021 (1999).
- [52] Z.-J. Wu *et.al.*, Phys. Rev. B **71**, 205323 (2005).
- [53] X.-T. Liang, Phys. Rev. B **72**, 245328 (2005).
- [54] S. Vorojtsov, Phys. Rev. B **71**, 205322 (2005).
- [55] Z.-Z. Li, X.-Y. Pan, X.-T. Liang, Physica E **41**, 220 (2008).
- [56] J. Gilmore, R.H. McKenzie, J. Phys.: Condens. Matter **17**, 1735 (2005).
- [57] C.M. Niemeyer, Curr. Opinion. Struct. Bio. **4**, 609 (2000).
- [58] J. Gilmore, R.H. McKenzie, Chem. Phys. Lett. **421**, 266 (2006).